Hemicelluloses extraction and nanocellulose addition as a partial replacement for non-renewable adhesives in oriented strand board.

by

Marina Natalia Hornus

A thesis submitted to the Graduate Faculty of
Auburn University
in partial fulfillment of the
requirements for the Degree of
Master of Science

Auburn, Alabama
May 5, 2019

Keywords: wood adhesive, hemicelluloses extraction, nanocellulose methylene diphenyl diisocyanate, oriented strand board

Approved by
Brian K. Via, Director of the Forest Products Development Center and Regions Bank Professor, School of Forestry and Wildlife Sciences, Auburn University
Maria S. Peresin, Assistant Professor School of Forestry and Wildlife Sciences, Auburn University
Thomas V. Gallagher, Professor, Forest Operations,
School of Forestry and Wildlife Sciences, Auburn University

Abstract

Oriented strand board (OSB) is an engineered wood product used for building wood-based structures (e.g., walls, floors, ceilings, furniture). This composite is manufactured with small pieces of wood (strands) linked together with adhesives and wax, which is added to reduce water absorption.

Wood composites are an alternative for satisfying the increased demand for building products and there are several advantages over solid wood. Similarly, to other wood composites, one of the main disadvantages of OSB is the absorption of environmental moisture. Therefore, the applications of wood-composite material are mainly limited by their irreversible thickness swelling. In order to make wood-based panels usable for exterior applications, it is necessary to improve their dimensional stability in high relative humidity conditions. Thus, the first investigation in this work was the pre-treatment of wood strands to increase the hydrophobic performance in final wood-based panels. The hypothesis was that the reduction of hydroxyl groups in wood strands would increase the dimensional stability of OSB. The literature suggests different pre-treatment to reduce hydroxyl groups in wood material. In the present work, pressurized hot water extraction was used, and three different conditions were tested (120, 140 and 160 ºC at 45 min). After wood strand pre-treatment, OSB samples were manufactured and static bending, internal bond, thickness swelling, and water absorption properties were tested using the ASTM D1037 procedures.

As a benefit to OSB manufacturers, project results have shown that removal of hemicelluloses with pressurized hot water increases the dimensional stability of the final wood

composite. This is attributed to less available hydroxyl groups associated to the presence of hemicelluloses. The pre-treatment at 160 °C resulted in the maximum amount of hemicelluloses extraction and OSB produced with this pre-treated material had the best dimensional stability. The percentage of extracted material increased as reaction temperature increased in the range of temperatures studied. At 120 °C, the percentage of hemicelluloses extracted was reduced but its impact on final OSB mechanical and physical properties was insignificant.

The second investigation in this work was the partial replacement of non-renewable polymeric methylene diphenyl diisocyanate (pMDI) adhesive by cellulose nanofibrils (CNF) in OSB. The demand for wood composites has been increasing and consequently so has the demand for pMDI. This has led to several efforts towards replacing non-renewable adhesives with renewable biomaterials. CNF has a high modulus of elasticity; therefore, it could be an opportunity to reinforce and partially replace the pMDI adhesive in OSB. In this work, two experimental designs at different density were conducted, each one with two factors (adhesive and CNF), and three levels (2.7, 4.4, and 6.2 % for adhesive and 0, 3, and 6 % for CNF). Static bending, internal bond, thickness swelling, and water absorption properties were tested on OSB samples using the ASTM D1037 procedures. The result showed that for most of the properties, the CNF did not have a statistically significant effect at the 95.0 % confidence level, for some properties, the effect was positive and for the internal bonding, the effect was negative. For the adhesive result showed that for most of the properties, it had a statistically significant positive effect at the 95.0 % confidence level. The more adhesive was added the better the properties were observed.

Acknowledgments

First and foremost, the person who invited me as a visiting scholar and believed in me from the beginning and has been my biggest supporter before, during, and after the process of performing my master's degree deserves the most acknowledgment Dr. Maria Soledad Peresin.

Second, I would like to give a special thanks to Dr. Brian Via, not only for the opportunity given to me when he accepted me for a master's position but also because of his guidance and patience, especially with my English. Dr. Via, Dr. Peresin and Dr. Gallagher have supported me in the past two years.

A special thanks to Shaoxuan Li for all the support, love, and guidance since the day we have met. I would like to thank my friends Celeste Iglesias, who always provided a helping hand and for being my companion, often late in the lab.

Finally, I want to show my gratitude to people who were always there for me even from thousands of miles away: my father Guillermo, mother Ana and siblings Cristina, Adela, Daniel and Camila and my friend Horacio Fernandez.

Table of Contents

List of Tables

List of Figures

List of Abbreviations

CNF cellulose nanofibrils

HW hardwood

IB Internal Bond

MDI Methylene Diphenyl Diisocyanate

MOE Modulus of Elasticity

MOR Modulus of Rupture

OSB Oriented Strand Board

PF phenol–formaldehyde

pMDI Polymeric Methylene Diphenyl Diisocyanate

SW softwood

TS Thickness Swelling

UF urea–formaldehyde

WA Water Absorption

Chapter 1

1.1. Introduction

Engineered wood product is a term used to describe all products manufactured by binding together wood materials such as strands, particles, fibers or veneers with adhesives. These products are an alternative for satisfying the increased demand for building materials and there are several advantages over solid wood (Hammett and Youngs 2002). One of the important advantages of wood composites is that it has more consistency overall, due to defects being more distributed within the composite. Although average mechanical properties for wood composites are generally lower than natural lumber, they exhibit much less variability that allows for better prediction by engineers. The mechanical properties of wood-based composites are derived from the particulate nature of the wood raw material (Youngquist 1999). The use of wood products contributes to carbon sequestration because wood is a renewable and organic material, meaning that carbon is the key component (Youngquist 1999).

Wood composites can be divided in two categories based on their end applications: non-structural applications such as oriented strands board (OSB), particleboard and fiberboard; and structural application such as glulam, laminated veneer lumber (LVL), oriented strand lumber (OSL), parallel strand lumber (PSL) and scrim-based lumber (Walker 2006).

This research is focused on OSB due to the increased use as a low-cost alternative to plywood (Lippke and Edmonds 2006). Since OSB is processed from small pieces of wood, it can efficiently utilize small trees and underutilized logs.

1.2. International trends in OSB

The United States is the main net importer of wood-based panels (OSB, particleboard, and fiberboard), followed by Africa. The five largest producers of these panels are China, United States, Russia, Canada, and Germany. They account for 69 percent of global production, and China represents 51 percent of this amount. The four important consumers of wood-based panels are the same as the four main producers, indicating that the products are mostly consumed internally. The five largest exporters are China, Canada, Germany, Russia and Thailand (FAO 2016). Figure 1.1 represents the top 10 manufacturers of wood-based panels around the world.

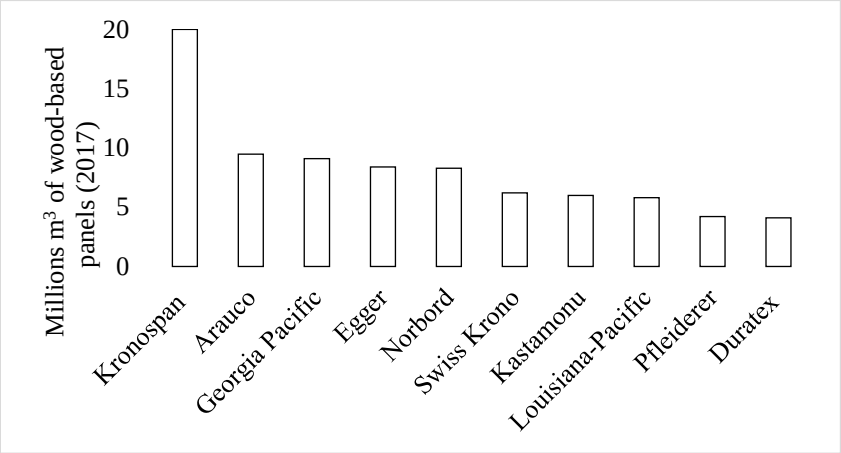

Figure 1.1. Main producers of wood-based panels. Information adapted from Arauco estimations and company information and filings. Hawkins Wright (2017)

The production of OSB started in North America in 1965 (Benetto et al. 2009). Nowadays, this wood-based panel dominates the marketplace in this country, where it passed plywood production in 1999 (Hansen 2006). The reason behind the fast growth in OSB production is due to the increased use of OSB as a low-cost alternative to plywood (Lippke and Edmonds 2006). As the OSB industry learned to control process variables such as the size of wood strands and orientation of them in different layers, the performance and outstanding mechanical properties of OSB products have been enhanced to the point where they are as good

as plywood in many performance categories. Consequently, OSB started to replace softwood plywood in construction applications (Stark 2010). In addition, a limited quantity of large log supplies in many countries has led to a drop in plywood manufacturing, which, in turn, contributed to the increased demand for OSB.

Europe has a lower production volume when compared to North America (Figure 1.2). Today, total OSB production in Europe is just over 8 million m^3/year, while in North America, it is approximately 20 million m^3.

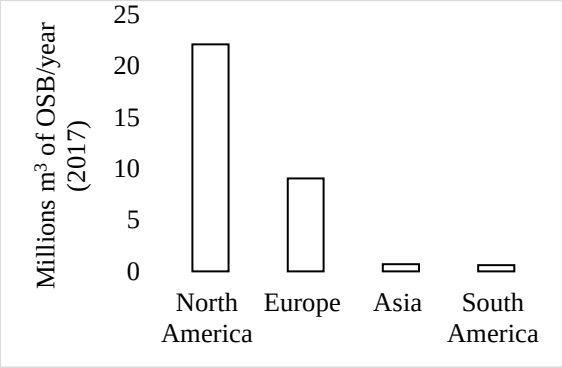

Figure 1.2. OSB capacity by region around the world. Information adapted from Wood Based Panels International (WBPI)

About 20 companies manufacture OSB in the United States, Canada, and Europe. Figure 1.3 shows the most important OSB companies from around the world.

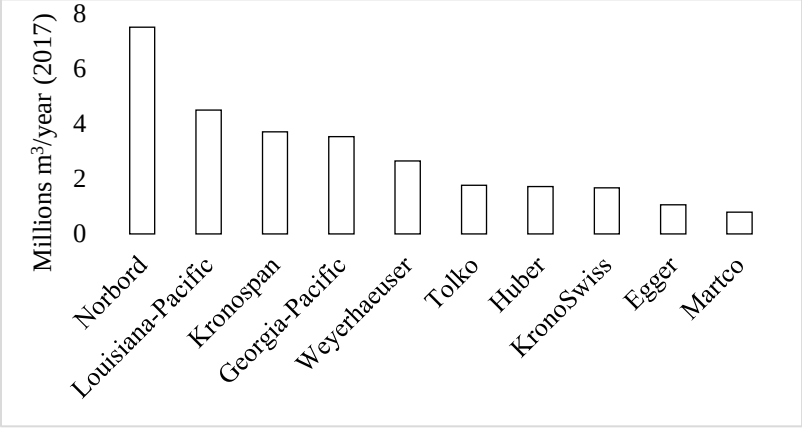

Figure 1.3. Top 10 global OSB companies. Information adapted from Wood Based Panels International (WBPI)

The global sales for OSB increased by 30 percent from 2012 to 2017, with an average growth rate of 6.5 % per year. Europe and North America are the main consumption regions. In 2016, these two regions occupied 90 % of the global consumption volume in total (Norbord 2018). The biggest company in OSB production in North America is Norbord (Figure 1.4), while in Europe it is Kronospan (Figure 1.5). Responding to the increased market demand, Kronospan is finishing its extension of an OSB board plant in Ufa, Russia. The factory is estimated to produce 1,000,000 m^3 /year of products, nearly doubling Kronospan's current production capacity (information from wood-based panels international).

Wood panel price depends on demand for building products, which is influenced by the economy, demographics and the need for housing. When there is a reduction in furniture sales and the number of houses that are built, there is an excess inventory resulting in a price drop. Wood panels are projected to grow faster than consumption and therefore consumption will need to expand to new markets as a precondition to not drop price due to excess inventory. Figure 1.6 displays the price of OSB in the last 14 years.

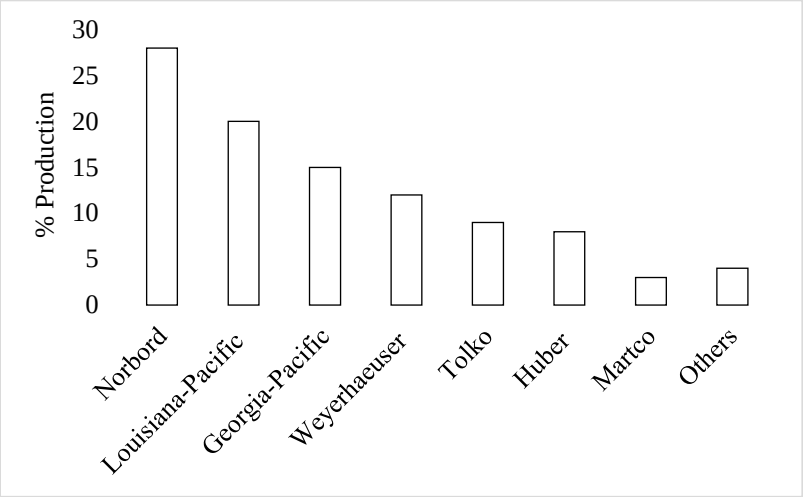

Figure 1.4. North America main OSB companies. Information adapted from Wood Based Panels International (WBPI)

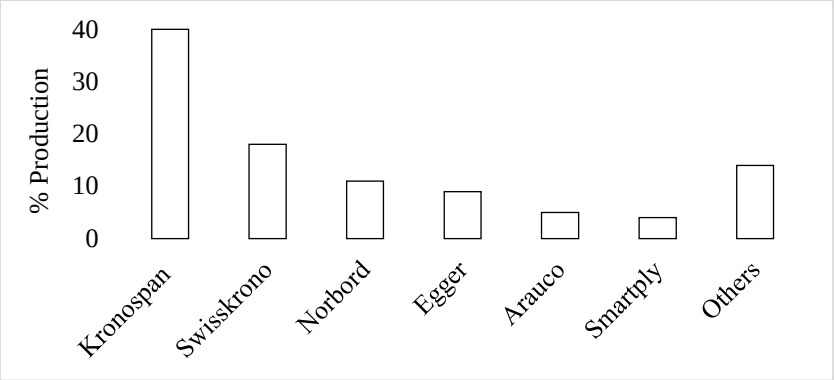

Figure 1.5. Europe main OSB companies. Information adapted from Wood Based Panels International (WBPI)

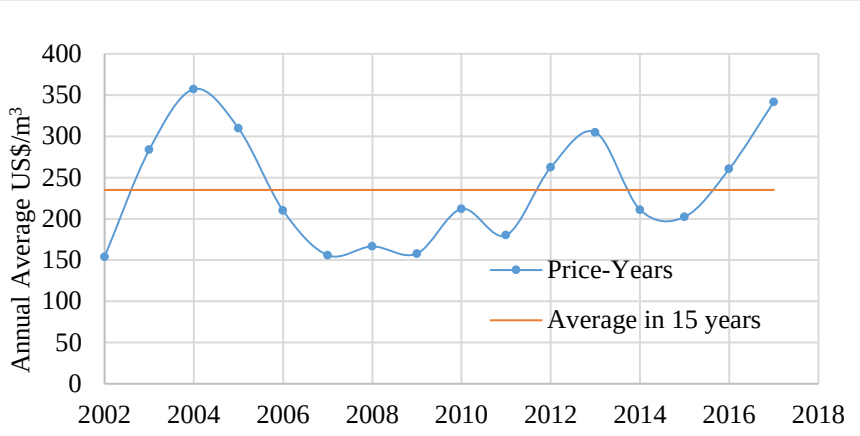

Figure 1.6. OSB price in the last 14 years. Information adapted from Investment report Norbord Company

1.3. Oriented strand board manufacturing

OSB is manufactured from fast-growing, small all trees. The manufacturing of OSB is described in Figure 1.7. During raw material preparation, logs are debarked prior to strand production. Generally, strand size is 11 cm in length, 3 cm in width, and 0.1 cm in thickness and smaller. After drying, the strands pass a screening step where they are divided into two groups;

larger strands for surface layers and smaller strands for the core. The orientation of the strands in the external layers is important to increase bending strength and they should be oriented longitudinal to the panel's main axis.

After drying and size classification, strands are transferred to blenders in which adhesives, sometimes wax, and other additives are sprayed onto strands from an atomizer to achieve a fine resin droplet size. The adhesive is used to bond wood strands together and the bonding strength has a great impact on final OSB panel strength. Resin dispersion, distribution, bond-line thickness, and resin penetration determine the final strength of composite (Gagliano and Frazier 2001). Different commercial resins are available such as urea–formaldehyde (UF), phenol–formaldehyde (PF), polymeric methylene diphenyl diisocyanate (pMDI), and melamine urea-formaldehyde (MUF). Wax is typically added at 0.3 – 1 % of the oven-dry weight of the strands for short-term moisture resistance (Youngquist 1999).

After chemical addition, strands are ready for mat formation. Mat formers can have different configurations, such as electrostatic equipment, mechanical devices containing spinning disks to align strands along the mat (Stark 2010). The formed mat is pressed under heat and pressure to a certain thickness to achieve a target density. The final density has a strong positive relationship with composite strength. The pressing step is critical and factors such as time, temperature, and pressure are the most important parameters. Hot pressing brings the surface particles together for bonding and provides heat to cure the adhesives. Two types of hot-presses are reported: batch hot-press and continuous hot-press. The total press time is approximately two and a half minutes for a continuous hot-press and up to 5 minutes for a multi-opening batch press. The operating temperature ranges from 140 °C to 220 °C. The hot-press is typically heated

by steam generated from a wood-burning boiler. After hot pressing, panels are cooled before finishing.

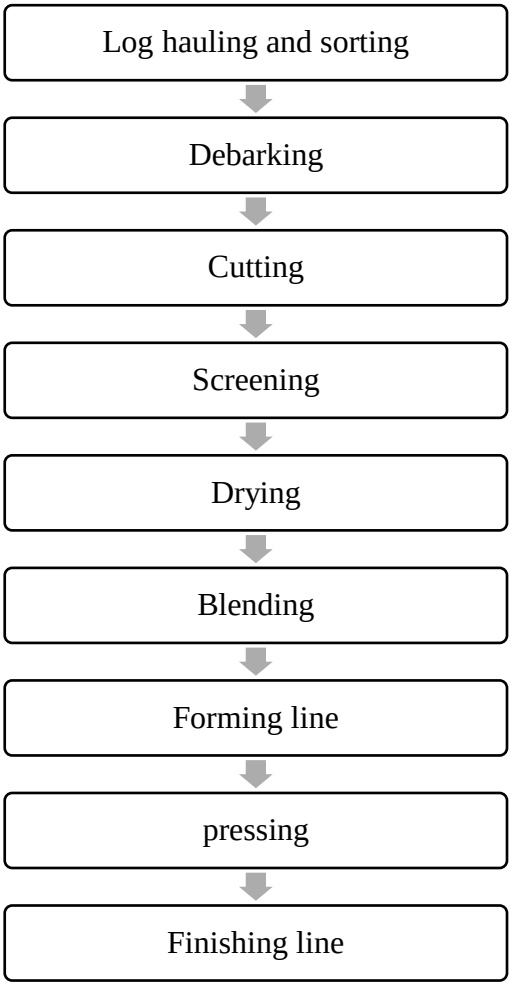

Figure 1.7. Oriented strand boards manufacturing flowchart

1.4. Oriented strand board test

The common properties of the wood composite that industry tests for are: modulus of rupture (MOR), modulus of elasticity (MOE), internal bonding (IB), thickness swelling (TS) and water absorption (WA). Industries within the U.S. follow the procedures of the American Society for Testing and Materials ASTM D1037 (ASTM 2012).

For measuring the MOE, MOR, and IB a Static Material Testing Machine is used (MTS universal testing machine Zwich/Roell Z010). MOR and MOE are tested in dry and wet conditions. For wet conditions, OSB samples are soaked for 24-hours continuously and then tested for mechanical properties. Figure 1.8 is an example of a sample being tested for MOR and MOE. For these tests, samples are loaded with longer strands facing down to ensure maximum breaking force and consistency between tests.

Figure 1.8. OSB sample being tested in the Z010 static material tester

Modulus of rupture is calculated using the following equation:

$$Rb = \frac{3\ L\ Pmax}{2\ b\ d^2} \tag{1.1}$$

where Pmax is the maximum load (N), b is the width of the specimen (mm), d is the thickness of the specimen (mm), L is the length of span (mm) (ASTM 2012).

The modulus of elasticity is a measure of stiffness. Higher MOE in wood composite, which is desired, indicates plastic deformation, while lower MOE shows elastic deformation. Modulus of elasticity is calculated using the following equation:

$$E = \frac{L^3}{4\ b\ d^3}\frac{\Delta P}{\Delta y} \tag{1.2}$$

where $\Delta P/\Delta y$ is the slope of the straight-line portion of the load-deflection curve (N/mm) (ASTM, 2012).

Internal bond strength is described as a tension test perpendicular to the surface of the specimen. The IB is calculated using equation 1.3. In this test, samples have to be 5 cm square, and the thickness should be that of the finished panel. Samples are glued with aluminum blocks to each of the square faces of the specimen and then loading in the fixture on the Zwick/Roell Z010 Static Material Testing Machine for testing (ASTM 2012) as shown in Figure 1.9.

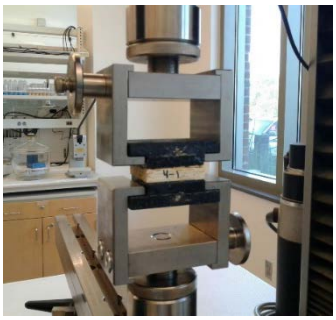

Figure 1.9. OSB sample being tested the internal bond strength

$$IB = \frac{P_{max}}{a\ b} \qquad (1.3)$$

where P_{max} is the maximum load (N), a is the width of the specimen measured (mm), and b is the length of the specimen measured (ASTM 2012).

Thickness swelling and water absorption are determined by soaking samples (ASTM 2012). Samples are immersed in tap water for 24 hours (Figure 1.10.a) and special care is taken to prevent samples from floating. Wire netting and weights are used to fully submerge the samples in water. Water is maintained at a level of 25 mm above the specimens while soaking. For each sample, the thickness is measured in four pre-marked and equally spaced points, at the midpoint of each side, and 2 cm from the edge as shown in Figure 1.10.b. The thickness is measurement before and after soaking samples. Amount of water that samples absorbs is determined weighting samples before and after soaking as shown in Figure 1.10.c.

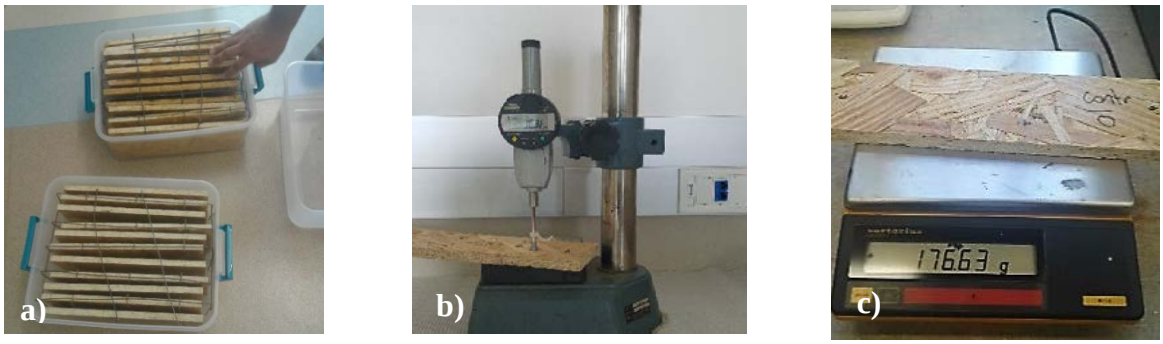

Figure 1.10. Determination of dimensional stability on OSB samples

Thickness swelling percentage is calculated as the difference between the average thickness before and after soaking samples (equation 1.4).

$$\%\text{Thickness swelling} = \frac{t_2}{t_1} * 100 - 100 \qquad (1.4)$$

where t_2 is the average thickness of 4-point measurement after 24 hours of soaking, and t_1 is the average thickness of 4-point measurement before 24 hours of soaking.

Water absorption percentage is calculated as the difference in mass before and after soaking samples (equation 1.5).

$$\%\text{Water absorption} = \frac{\text{Final weight- Initial weight}}{\text{Initial weight}} * 100 \qquad (1.5)$$

1.5. Pressing theory

Several types of presses can be used in the manufacturing of oriented strand board: batch or continuous, plate, steam injection, and/or radio frequency or micro-wave heated (Sturgeon et al. 1989).

Physical, chemical, and mechanical phenomena are present in the pressing process. Pressing strand board is primarily controlled by pressure and temperature for a specified time (Bolton and Humphrey 1988; Hata et al. 1990; Kamke and Wolcott 1991; Suo and Bowyer 2007). Heat and mass transfer are the main transport mechanism in this process. The heated press

platens evaporate the bound water of the strands at the surface during the initial stage of pressing. This built up vapor pressure that drives the evaporated water to the cold center of the mat. This vapor would then condense in the cold mat center. The core temperature would gradually increase, and the water in the core would eventually vaporize. The increased vapor pressure would then drive the vapor to the surface, or outside boundary, of the mat and exit the mat (Zombori et al. 2001). This steam flow assists heat transport but would subside as the water content of the mat is depleted. The rate of moisture and heat transfer depends on the structure geometry of the mat and how it is altered during the compression. A void volume occurs as a result of the compression process and flake geometry that always varies and creates a pathway for fluid flow. Thermal conductivity, permeability, and diffusivity of the mat are changing during the pressing process (Zombori et al. 2001). The density of the mat has a direct influence on the void volume.

1.6. Polymeric Methylene Diphenyl Diisocyanate (pMDI) and adhesion theory

Commercial pMDI is a mixture of aromatic monomer and polymeric of diphenyl methane diisocyanate (MDI and pMDI respectively). Typically it consists of about 30 % tri-isocyanate, 10 % tetra-isocyanate, 5 % penta-isocyanate, 5 % higher homologue, and 50 % pure MDI, of which, approximately 95 % is 4,4’-methylene-diphenyl-diisocyanate (Frazier 2003).

In wood composites, pMDI is commonly referred to as MDI. The isocyanate adhesive is primarily used to produce OSB and other related strand products. MDI reacts very aggressively with the many hydroxyl groups available in wood.

The advantage that pMDI has compare to other adhesives is moisture tolerance. High moisture tolerance is wanted because it means less drying time with minor energy costs and lower emissions of volatile organic compounds. Panels that use pMDI can contain up to 10-15%

of moisture while panels with liquid PF resins only up to 4-5 %. Another advantage of pMDI is that it does not emit formaldehyde, and due to the recent concerns about formaldehyde use, many OSB companies are using pMDI more than phenol formaldehyde in recent years. However, pMDI is dangerous during the manipulation process and special cares are necessary to avoid direct contact with this chemical. One more disadvantage of pMDI is that it adheres intensely to nearly all surfaces (Sonnenschein and Wendt 2005). Therefore, external release agents are required to avoid adhesion between press plates and panels. In the past, this disadvantage has inhibited the growth of pMDI in the OSB industry due to the additional cost of the release agent.

The polymeric MDI is an organic brown liquid whose viscosity depends on the molecular weight of the polymer and the frequency of the 3-ring. Viscosities of pMDI are approximately 0.18–0.25 Pa s (170–255 cP) and the surface tension is approximately 40–45 mN/m. That means pMDI is low in molecular weight, viscosity, and surface tension. Therefore, pMDI can readily wet and penetrate deep into the wood. Polymeric MDI flows into the micrometer size voids of wood via capillary action. In addition, pMDI contains no water so it cannot lose its mobility by absorption on the wood surface by physical bonding. Apparently, penetration occurs down to the angstrom scale. In other words, pMDI penetrates into the amorphous regions of the wood cell wall. The adhesion force of covalent and physical bonding is related to the amount of surface area contact between the adhesive and the cell wall (Kamke and Lee 2007). Greater flow along the lumen surfaces means more potential for chemical bonds to form.

Polymeric MDI has a density of 1.23 g/cm^3 at 25 °C. It tolerates high temperatures and has a low flammability risk due to its flash point of over 200 °C. It starts to decompose at temperatures above 230 °C. The synthesis of diphenylmethane diisocyanate and its homologue is a complex process. It is produced from a condensation reaction between aniline and

formaldehyde, using hydrochloric acid as a catalyst. Three possible isomers (4,4'-, 2,4'-, and 2,2'), of methylenedianiline are formed during the reaction between one mole of formaldehyde and two moles of aniline. The diamine isomers then react with phosgene. The phosgenation reaction converts the amino groups into isocyanate (Twitchett 1974). Afterward, this mixture is split into polymeric MDI and pure MDI (Figure 1.11). Pure MDI consists mainly of two isomers: 2,4'-MDI and 4,4'-MDI

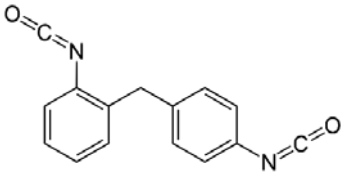

2,4'-MDI

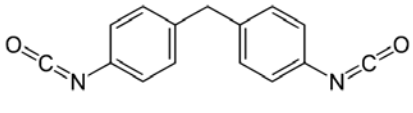

4,4'-MDI

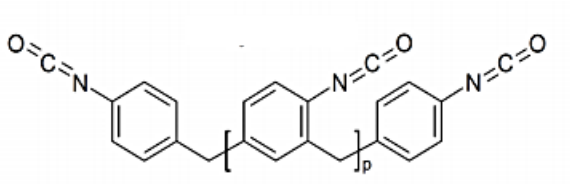

Polymeric MDI

Figure 1.11. Two frequent MDI isomers, and the polymeric MDI structure.

The reactivity of the isocyanate groups (NCO) depends on its positions. The NCO in 2 (ortho)-position is three times less reactive than the isocyanate group in 4 (para)-position. Therefore, 4,4'-MDI is more reactive than 2,2'-MDI. Furthermore, on average, pMDI is less reactive than the pure 4,4'-MDI because the oligomeric polyisocyanates have ortho substituted NCO groups. Pure 4,4'-MDI is a major raw material for adhesive and coating applications where high reactivity is required, it is solid at room temperature and melts at 38 °C (Gurke 2002). The commercial MDI is a mixture of 2,4'-MDI, 4,4'-MDI and polymeric MDI. This is storage stable and no crystallization takes place down to temperatures of 0 °C.

The reaction of the MDI occurs because its isocyanate groups can react with primary and secondary amines, primary alcohols, water, secondary alcohols, and phenols. The relative reactivity of these compounds with isocyanate depends upon the nucleophilicity and steric structure. Regarding the isocyanate group, it presents variable reactivity depending on the position in the pMDI.

In theory, isocyanate groups from pMDI can react with wood hydroxyl groups and water hydroxyl groups. The reaction of isocyanate groups with hydroxyl groups from wood produces irreversible urethane linkages (Figure 1.12).

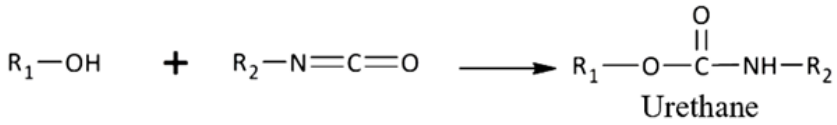

Figure 1.12. Reaction between a hydroxyl group from wood and isocyanate group to produce urethane linkage

Then the secondary amine in the urethane can react with other isocyanate groups to form allophanate bridges (Figure 1.13). This continues the crosslinking and hardening of the adhesive.

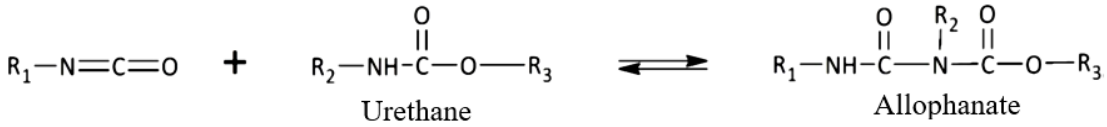

Figure 1.13. The reaction of an isocyanate and urethane to form an allophanate bridge

On the other hand, the reaction between isocyanate groups and water produces carbamic acid, which quickly degrades into an amine with carbon dioxide gas being released (Figure 1.14).

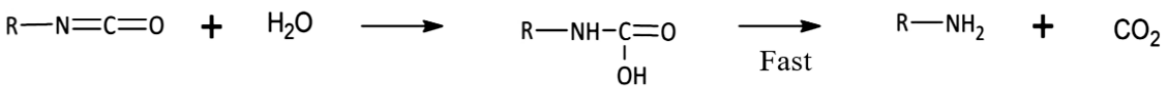

Figure 1.14. The reaction of isocyanate and water producing a primary amine

Then the produced amine reacts with other isocyanate group and produces a urea molecule (Figure 1.15).

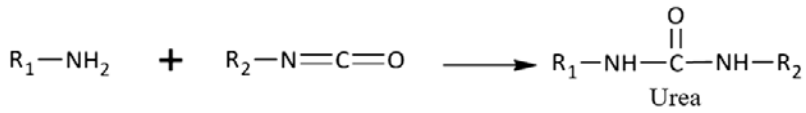

Figure 1.15. The reaction between primary amine and isocyanate producing urea

This substituted urea can then react with other isocyanate groups to produce biuret bridges (Figure 1.16). These biuret bridges also strengthen crosslinking and help harden the cured adhesive (Frazier 2003).

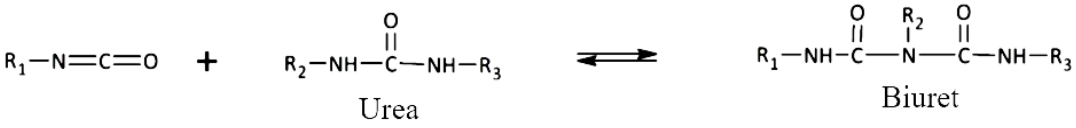

Figure 1.16. Reaction between an isocyanate group and urea producing biuret linkage

Hydrogen bonding that promotes strong secondary interactions is typical between urethane and urea. The N-H group acts as a proton donor while the carbonyl acts as a proton acceptor (Figure 1.17). Hydrogen bonding between these groups increased the bonding strength of the adhesive (Wang 1998).

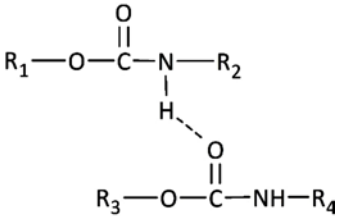

Figure 1.17. Hydrogen bonding between urethane groups

In primary bonds, the covalent chemical bonding theory is the prevailing theory thought to be present with adhesives, but it is difficult to prove. Under normal conditions, the formation of covalent bonds between adhesive and wood substrates has never been observed (We 1989). It is either not present or undetectable because there is a low proportion of covalent bonds compared with other bonds. Therefore, the author concludes that covalent bonding between resin

and wood is either absent or negligible. Polymeric diphenyl methane diisocyanate (pMDI) had been assumed to covalently bond with the hydroxyls of the wood substrate, but We (1989) concludes that there is no covalent bonding between pMDI and the wood substrate due to the more likely reaction of pMDI with water. The reaction of isocyanates from pMDI with water to form polyurea proceeds at 7.4×10^{-6} l mol^{-1} s^{-1}, while hydroxyls from wood carbohydrates to form polyurethane proceeds at 2×10^{-7} l mol^{-1} s^{-1}, and aliphatic hydroxyl groups such as is found in lignin to form polyurethane proceeded at 6×10^{-6} l mol^{-1} s^{-1}. This demonstrates that isocyanates are more likely to react with water to form polyurea rather than with hydroxyls from wood to form polyurethane. Polyurea from the reaction of pMDI and water are shown to adhere to the wood substrate by secondary forces alone (Frisch et al. 1983). The adsorption/specific adhesion theory claims that an adhesive adheres to a substrate due to the intermolecular and interatomic forces between atoms and molecules of the two materials (Pizzi 1994; Browne 1929). Pizzi (1994) concludes that intermolecular and interatomic forces such as hydrogen bonds, electrostatic interactions, and van der Waals interactions are the dominant mechanism for bonding wood. Therefore, the adsorption/specific adhesion theory is the primary theory of adhesion assumed in this research with wood adhesives due to primarily van der Waals forces and hydrogen bonding.

There are three potential failure mechanisms with wood adhesives. The possible failure points are in the wood/adhesive interface, the adhesive itself, or the wood itself. The different zones (Figure 1.18) that are associated with the wood and adhesive interaction, as well as the defect associated with the wood/resin interface, are described by Marra. Region 1 represents the pure adhesive. It is considered cohesive failure in this zone, and the adhesive is deemed not acceptable if this is the point of failure. The adhesive boundary is represented by Regions 2 and 3

and it is considered the beginning of the interphase region. Regions 4 and 5 represent the interface of the boundary layer and substrate. This is where the primary adhesive mechanism is represented. Regions 6 and 7 represent the wood cells modified by the adhesive. This is the surface of the wood where resin penetration drives the mechanism. The adhesive is considered acceptable if a failure occurred here. Regions 8 and 9 are unadulterated wood.

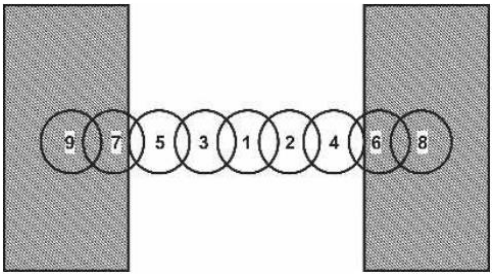

Figure 1.18. Chain link analogy for an adhesive bond in wood (Marra 1992).

The wood/resin interface has three stages of adhesion: bond-forming, liquid to solid, and durability. Bond forming is dependent on rheological properties and thermodynamic wetting. The substrate should have higher surface energy than the adhesive and must make contact on the molecular level to form a bond. Penetration of the adhesive into the substrate is related to the good bond formation and is thought to occur in wood either through the lumen or cell wall. Penetration in the lumen depends on the viscosity of the adhesive, applied pressure, temperature, and time (McBain and Hopkins 1925). High viscosity adhesives may not wet well especially with substantial microroughness of the substrate (Pocius 1997). Wetting of the adhesive must occur before higher viscosity from solidification of the adhesive hindered the wetting.

The liquid to a solid stage of adhesion involves polymerization, loss of solvent, and solidification from the melt. Durability involves the de-bonding process, which is due to viscoelastic energy dissipation. This can occur in all portions of the product (not just the wood-

adhesive interface) and is also influenced through dimensional changes in the wood (Frihart 2004).

1.7. Chemical composition in wood

Wood is comprised mainly by the structural components of cellulose, hemicelluloses, and lignin. These components together form the basic units of the cell wall and they are tightly bound through chemical and non-chemical forces. Cellulose is a linear homopolysaccharide consisting of D-glucopyranose units linked by β-1,4- glycosidic bonds. Hemicelluloses are heterogeneous polysaccharides composed of D-xylose, D-mannose, D-glucose, D-galactose, L-arabinose, and small amounts of D-glucuronic acid, 4-O-methyl-D-glucuronic acid, and D-galacturonic acid. Apart from the structural components, wood has low-molecular-weight component known as extractives. They are present in minor fractions mostly <10 % of the dry wood weight.

The proportions of the components in wood vary from species, geographic locations, soils, weathers, and within the same tree. Wood species are divided into two groups commonly known as softwood (SW) and hardwood (HW). Differences between softwood and hardwood not only lies in the percentage of the amount of cellulose, hemicelluloses, and lignin but also the composition of the hemicelluloses and lignin (Table 1.1). In addition, the fiber length in softwood is 2-6 mm, while in hardwoods it is 0.8-1.6 mm (Solala 2015).

Table 1.1. Wood chemistry composition in percentage of dry weight (Sjöström 1993)

Wood	Cellulose	Hemicelluloses			Lignin	Extractives
		Galactoglucomannans	Xylan	Glucomannan		
Softwood	37-43%	15-30%	5-10%		23-33%	2-5%
Hardwood	39-45 %		15-30%	2-5%	20-25%	2-4%

Cellulose constitutes 40-50 % of the dry weight of lignocellulosic biomass. The polymer chain is composed of β-1,4- glycosidic bonds linked D-glucopyranose units in which the repeating unit is cellobiose that is a two-unit sugar (Figure 1.19). The degree of polymerization is about 10,000 (based on the wood cellulose) (Sjöström 1993; O'Sullivan 1997; Klemm et al. 2005).

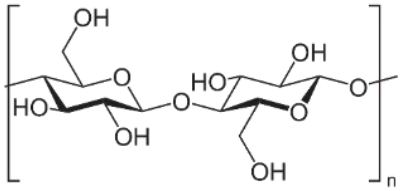

Figure 1.19. Cellulose chain structure

Existing as completely unbranched homopolymers, cellulose molecules form microfibrils by hydrogen bonds. The three OH groups present in each anhydroglucose are able to interact with hydroxyl groups from other anhydroglucose units forming inter and intramolecular bonds within and between cellulose chains conferring rigidity, stability, and water insolubility to the cellulose (Moon et al. 2011). The intramolecular H-bonds occurring from O(3)-H to O(5) and O(2)-H to O(6), and the intermolecular H-bond taking place from O(3)-H to O(6)-H.

Based on the arrangement and hydrogen bonds within and between the cellulose chains, different crystalline allomorphs cellulose I, II, IIII, IIIII, IVI, and IVII exist that can be interconverted, by chemical or thermal treatments (Habibi et al. 2010). Within the cell wall, cellulose can be present as crystalline and non-crystalline. The non-crystalline or amorphous regions are more accessible to water, chemicals or microorganisms. The crystallinity of cellulose makes it extremely stiff as well as hydrophobic (Kondo et al. 2001; Rowel 2016; Sjöström 1993).

Cellulose is further organized by forming elementary fibrils with diameters between 3-5 nm so elementary fibrils are a bundle of 50 to 80 cellulose molecules. Elementary fibrils are combined into larger structures called microfibrils with diameters between 10 to 20 nm, which are further arranged together in a fibril-matrix like structure mixed with hemicelluloses and lignin that can be found on the cell wall layers (Postek et al. 2011). The cellulose microfibrils give stiffness to the wood in the longitudinal and transversal directions, as cellulose has a higher elastic modulus compared to hemicelluloses or lignin. Cellulose microfibrils will not associate with lignin but will bind with hemicelluloses.

Hemicelluloses associate with both lignin and cellulose in the cell wall. The hemicelluloses act as a matrix for the cellulose microfibrils. Together the cellulose microfibril in hemicelluloses matrix is referred to as holocellulose. The lignin acts as an encrusting agent for the holocellulose fraction of wood. In theory, the hemicelluloses matrix acts as an adhesive between the cellulose microfibrils and surrounding lignin. Acting as adhesive, hemicelluloses do not impart much tensile strength to wood material, but lignin provides strength in both compression and shear.

Enzymatic hydrolysis has been established that hemicelluloses are principally located between the cellulose microfibrils in the cell wall structure, while remaining hemicelluloses have been suggested to be within the amorphous region of the cellulose microfibrils structure (Arola et al. 2013).

After cellulose, hemicelluloses are the most abundant biopolymers on earth. Hemicelluloses make up 20-30 % of the dry wood weight. The polymerization degree of hemicelluloses is only around 200. This lower degree of polymerization when compared with cellulose (10,000) makes hemicelluloses more soluble (Sjöström 1993). Unlike cellulose,

hemicelluloses are branched heteropolysaccharides and can be easily hydrolyzed by acids to their corresponding monosaccharides which are mainly composed of pentoses (D-xylose, D-arabinose), hexoses (D-mannose, D-glucose, -galactose) and sugar acids (Klemm et al. 2005; Tunc and Van Heiningen 2008). The amorphous and branched structures of the hemicelluloses confer to them more accessibility to chemical reaction, water uptake, and microorganisms attack when compared with cellulose (Jingjing 2011).

The hemicelluloses in softwoods and hardwoods differ in composition and quantity. Hardwoods hemicelluloses are rich in xylans polymers with a small amount of mannan, while softwood hemicelluloses are rich in mannan polymers (Kumar et al. 2008; Sjöström 1993). In both softwood and hardwood, acetyl groups often substitute the hydroxyl groups at C-2 or C-3 positions on the backbone chains of hemicelluloses, although softwoods are normally less acetylated than hardwoods. Side groups on hemicelluloses prevent the formation of crystalline regions.

In hardwood hemicelluloses, the major chains are typically glucuronoxylan (15-30 % of the dry wood), made up of β-1,4-linked D-xylopyranose units, with 4-O-methyl-α-D-glucuronic acid linked to the main chain about every ten xylose residues by 1,2- bonds (Sjöström 1993). In softwood hemicelluloses, the principal backbone chains are galactoglucomannan, arabinoglucuronoxylan, and arabinogalactan, with galactoglucomannan the principal one (Sjöström 1993). Galactoglucomannan, as the name suggests is constituted by galactose, glucose, and mannose. The backbone is built up by β-1,4-linked D-glucopyranose and β-D-monnopyranose units (Figure 1.20) where the C-2 and C-3 of mannose and glucose units are partially substituted by acetyl groups, on the average one group per 3-4 hexose units.

Galactoglucomannans hemicellulose can have a different amount of galactose unit and they are easily depolymerized by acids (Sjöström 1993).

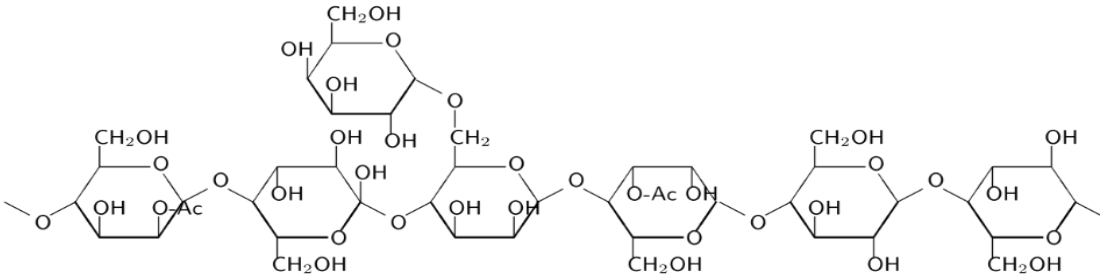

Figure 1.20. The basic structure of galactoglucomannans main hemicellulose in softwood.

Arabinoglucuronoxylans are present about 5-10 % in softwood. The backbone is β-1,4-linked D-xylopyranose units which are partially substituted at C-2 by 4-O-methyl-α-D-glucuronic acid group, on the average two residues per ten xylose units. In addition, the backbone contains -α-L- arabinofuranose units, on the average 1.3 residues per ten xylose units. Arabinogalactan is water-soluble hemicelluloses. Its backbone is built up by β-1,3-linked D-galactopyranose units. Almost every unit carries a branch attached to position 6, largely β-1,6-linked D-galactopyranose residues but also L-arabinose. There are also a few glucoronic acid residues present in the molecule. The highly branched structure is responsible for the low viscosity and high solubility in water of this polysaccharide (Sjöström 1993).

Lignin is the third abundant biopolymer in nature. It is the less hydrophilic component of the wood. Softwood contains 26-32 % lignin while hardwood normally contains 20-25 % lignin (Sjöström 1993). All vascular terrestrial plants produce lignin, which is large amorphous and branched three-dimensional polymers of phenylpropane units (Chakar and Ragauskas 2004). C-O-C and C-C linkages between the monolignols, p-coumaryl alcohol, coniferyl alcohol, and sinapyl alcohol (Figure 1.21) make up the three-dimensional structure (Sjöström, 1993; Rowel 2016).

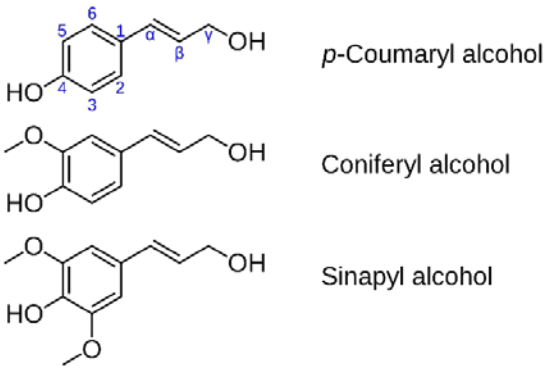

Figure 1.21. The three lignin precursors

Even though lignin has been studied for decades, the exact original chemical structure remains unknown. It is believed that lignin chemically binds to carbohydrates, forming lignin-carbohydrates complexes (LCC) possibly through ester and ether or even glycosidic bonds (Sjöström 1993). The bond types are include β-O-4, α-O-4, β-5, 5-5, 4-O-5, β-1 and β-β, among which β-O-4 makes up over 50 % of wood lignin linkages.

Lignin is primarily obtained as a byproduct in wood pulping processes with estimates exceeding 75 million tons per annum. Therefore, great interest exists for possible applications such as in wood-based panels industry (adhesives, additive for part replacement of adhesives, and raw material for synthetic resins).

1.8 Cellulose nanofibrils (CNF)

In natural materials such as wood and cotton, cellulose polymer is packed into fibrils with a diameter of 1.5–3.5 nm. These fibrils are referred to as elemental fibrils and they are further packed together with hemicelluloses to form what is known as microfibril with a diameter of 10–30 nm. The microfibrils are packed further into macroscopic fibrils with a diameter of about 100 nm and length about several hundred nm (Klemm et al. 2005). Macroscopic fibrils are part of the cellulose fibers that with lignin and hemicelluloses form the cell wall of the wood.

During the pulping process, the cell wall of wood is broken down into fiber bundles and singles. Then these fibers by mechanical disintegration can be transformed to cellulose nanofibrils (CNF), which is a renewable material that has 3–20 nm in diameter and microns long. CNF has received special attention for its high aspect ratio, high strength, low-density, and excellent mechanical properties (Spence et al. 2010; D Klemm et al. 2011; Moon et al. 2011).

The production of CNF is not new, it started in 1980 when cellulose pulp suspensions were refined under pressure (Turbak et al. 1983; Herrick et al. 1983). At that time, this process was inefficient and expensive because large amounts of energy were needed to produce this material (Ankerfors 2012). However, years of efforts made possible to obtain CNF in techno-economically feasible with the emergence of new technologies, and different pre-treatment such as enzymatic and chemical. Two types of equipment can be used for the production of CNF; (a) microfluidizer, where the cellulose pulp suspension is required to pass through a small chamber allowing the fracture of the fiber into smaller portions (Lavoine et al. 2012), and (b) supermasscolloider, where the suspension is ground when passing between a stationary and a rotating stone which allows breaking and delamination of the fibers.

CNF can be produced with bleached or unbleached pulp fibers. The fiber election will depend on what surface properties people are looking for. However, respect to an environmental point of view the production of unbleached cellulose nanofibrils is more environment-friendly since the processes of lignin removal as well as the following bleaching steps are no longer necessary (Rojo et al. 2015; Spence et al. 2010).

References

Alner, D. (1969). Aspects of Adhesion, vol. 5. University of London Press.

Ankerfors, M. (2012). Microfibrillated cellulose : Energy - efficient preparation techniques and key properties. Licentiate Thesis in the KTH Chemical Science and Engineering, Stockholm, Sweden.

Arola, S., Malho, J-M., Laaksonen, P., Lille, M., and Linder, M. (2013). The role of hemicellulose in nanofibrillated cellulose networks. Soft Matter. 9(4):1319–1326.

ASTM. (2012). D1037 Standard Test Methods for Evaluating Properties of Wood-Base Fiber and Particle Panel Materials. American Society for Testing and Materials, West Conshohocken, PA.

Benetto, E., Becker, M., and Welfring, J. (2009). Life Cycle Assessment of Oriented Strand Board (OSB): from Process Innovation to Ecodesign. Environmental Science and Technology. 43(15):6003–6009.

Bolton, A. and Humphrey, P. (1988). The Hot Pressing of Dry-formed Wood-based Composites Part I. A Review of the Literatlire, Identifying the Primary Physical Processes and the Nature of their Interaction. Holzforschung-International J. Biol. Chem. Phys. Technol. Wood. 42(6):403-406.

Browne, F. and Brouse, D. (1929). Nature of Adhesion between Glue and Wood: A Criticism of the Hypothesis that the Strength of Glued Wood Joints Is Due Chiefly to Mechanical Adhesion. Industrial and engineering chemistry. 21(1):80-84.

Chakar, F., and Ragauskas, A. (2004). Review of current and future softwood kraft lignin

process chemistry. Industrial Crops and Products. 20(2):131–141.

FAO (2016). Global Forest Products Facts and Figures.

Frazier, C. (2003). Isocyanate Wood Binders In: Handbook of Adhesive Technology. Revised and Expanded, A. Pizzi and KL Mittal. New York: Taylor and Francis (Marcel Dekker Inc.).

Frihart, C. (2004). Adhesive interaction with wood. Fundam. Compos. Process. Proc. a Work. 29–54

Frisch, K., Rumao, L. and Pizzi, A. (1983). Diisocyanates as wood adhesives. Wood Adhes. Chem. Technol. Ed. Pizzi, A. Marcel Dekker, Inc. New York, pp. 289–317.

Gagliano, J. and Frazier, C. (2001). Improvements in the fracture cleavage testing of adhesively-bonded wood. Wood and Fiber Science. 33(3):377–385.

Hammett, A. and Youngs, R. (2002). Innovative Forest Products and Processes: Meeting Growing Demand. Journal of Forestry. 100 (4):6–11.

Hansen, E. (2006). Structural panel industry evolution: Implications for innovation and new product development. Forest Policy and Economics. 8:774–783.

Hata, T., Kawai, S. and Sasaki, H. (1990). Computer simulation of temperature behavior in particle mat during hot pressing and steam injection pressing. Wood Science and Technology. 24 (1):65.

Herrick, F., Casebier R., Hamilton K., Sandberg K. (1983). Microfibrillated cellulose: morphology and accessibility. J Appl Polym Sci Appl Polym Symp. 37:797–813

Jingjing, L. (2011). Isolation of Lignin from Pulp. Bachelor thesis in the Saimaa University of Applied Sciences.

Kamke, F. and Lee J. (2007). Adhesive penetration in wood: a review. Wood and Fiber Science.

39(2):205–220.

Kamke, F. and Wolcott, M. (1991). Fundamentals of flakeboard manufacture: wood-moisture relationships. Wood Science and Technology. 25(1):57-71.

Klemm, D., Heublein, B., Fink, H-P., and Bohn, A. (2005). Cellulose: Fascinating biopolymer and sustainable raw material. Angewandte Chemie-International Edition. 44(22):3358–3393.

Klemm, D., Kramer, F., Moritz, S., Lindström, T., Ankerfors, M., Gray, D. and Dorris, A. (2011). Nanocelluloses: A New Family of Nature-Based Materials. Angewandte Chemie-International Edition. 5438–5466.

Kondo, T., Togawa, E., and Brown, M. (2001). "Nematic ordered cellulose": A concept of glucan chain association. Biomacromolecules. 2(4):1324–1330.

Kumar, R., Singh, S., and Singh, O. (2008). Bioconversion of lignocellulosic biomass: Biochemical and molecular perspectives. J Ind Microbiol Biotechnol. 35(5):377–391.

Lavoine, N., Desloges, I., Dufresne, A., and Bras, J. (2012). Microfibrillated cellulose – Its barrier properties and applications in cellulosic materials: A review. Carbohydrate Polymers. 90(2):735–764.

Lippke, B. and Edmonds, L. (2006). Environmental performance improvement in residential construction: The impact of products, biofuels, and processes. Forest Product Journal. 54(10):58-63.

Marra, A. (1992). Technology of wood bonding. Van Nostrand Reinhold.

McBain, J. and Hopkins, D. (1925). On adhesives and adhesive action. J. Phys. Chem. 29(2):188–204.

Moon, J., Martini, A., Nairn, J., Simonsen, J., and Youngblood, J. (2011). Cellulose

nanomaterials review: Structure, properties and nanocomposites. Chemical Society Reviews. 40(7):3941–3994.

Norbord, C. (2018). Investor Presentation. Company Norbord. Available online at: https://www.norbord.com/cms/wp-content/uploads/Q3-2018-Investor Presentation_FINAL.pdf; last accessed March 8, 2019

O'Sullivan, A. (1997). Cellulose: The structure slowly unravels. Cellulose. 4(3):173–207.

Pizzi, A. (1994). Advanced wood adhesives technology. CRC Press.

Pizzi, A., and Mittal, K. (2003). Handbook of Adhesive Technology. CRC Press.

Pocius, A. (1997). Adhesion and Adhesives Technology. Hanser.

Postek, M., Vladár, A., Dagata, J., Farkas, N., Ming, B., Wagner, R., Raman, A., Moon, R., Sabo R., Wegner, T., and Beecher, J. (2011). Development of the metrology and imaging of cellulose nanocrystals. Measurement Science and Technology. 22(2).

Rojo, E., Peresin, M., Sampson, W., Hoeger, I., Vartiainen, J., Laine, J., and Rojas, O. (2015). Comprehensive elucidation of the effect of residual lignin on the physical, barrier, mechanical and surface properties of nanocellulose films, Green Chemistry. 17:1853–1866.

Rowel, R. (2016). Handbook of Wood Chemistry and Wood Composites. Journal of Cleaner Production. (Vol. 110).

Sjöström E (1993). Wood chemistry-fundamentals and applications, 2nd edn. San Diego, Academic Press Inc.

Solala, I. (2015). Mechanochemical reactions in lignocellulosic materials. Dissertation, Aalto Universty.

Sonnenschein, M. and Wendt, B. (2005). Efficacy of polymeric MDI/Polyol mixtures for binding wood boards. Wood science and technology. 39:27–36

Spence, K., Venditti, R., Habibi, Y., Rojas, O., and Pawlak, J. (2010). The effect of chemical composition on microfibrillar cellulose films from wood pulps: Mechanical processing and physical. Bioresource Technology. 101(15):5961–5968.

Sturgeon, M. and Lau, N. (1989). Continuous pressing medium density fibreboard at Nelson Pine Industries New Zealand. Proceedings of the Washington State University International Particleboard/Composite Materials Series Symposium (USA).

Tunc, S., and Van Heiningen, A. (2008). Hemicellulose extraction of mixed southern hardwood with water at 150^{o}C: Effect of time. Industrial and Engineering Chemistry Research. 47(18):7031–7037.

Suo, S. and Bowyer, J. (2007). Simulation modeling of particleboard density profile. Wood fiber Science. 26(3):397–411.

Turbak A, Snyder F, Sandberg K (1983) Microfibrillated cellulose. US Pat 4,374,702 11:1–11.

Twitchett, H. J. (1974). Chemistry of the production of organic isocyanates. Chemical Society Reviews. 3(2):209–230.

Stark, N., Cai, Z., Carll, C. (2010) , Wood-Based Composite Materials, Panel Products, Glued-Laminated Timber, Structural, Composite Lumber, and Wood–Nonwood Composite Materials. Wood handbook: wood as an engineering material. USDA Forest Service.

Walker, J. (2006). Primary Wood Processing (2nd ed.). New Zealand. Springer.

Wang, F. (1998). Polydimethylsiloxane Modification of Segmented Thermoplastic Polyurethanes and Polyureas Polydimethylsiloxane Modification of Segmented Thermoplastic Polyurethanes and Polyureas. Thesis in the Faculty of the Virginia Polytechnic Institute and State University.

We, J. (1989). The chemical bonding of wood. Wood Adhesive Chemistry and Technology, Vol.

2. Marcel Dekker, New York, NY.

Youngquist, J. (1999). Wood-based Composites and Panel Products. Wood Handbook—Wood as an Engineering Material. Madison, WI : USDA Forest Service, Forest.

Zombori, B., Kamke, F., and Watson, L. (2001). Simulation of the Mat Formation Process. Wood

Fiber Science. 33(4):564–579.

Chapter 2

Effect of hemicelluloses extraction from softwood on oriented strand board performance

2. 1. Introduction

Oriented strand board is an engineered wood product used for building, and furniture. This material is increasingly used as a low-cost alternative to plywood (Cheng et al. 2018; Lippke and Edmonds 2006). Similarly, to other wood composites, one of the main disadvantages of OSB is the absorption of environmental moisture. Therefore, the applications of wood-composite materials are often limited by their irreversible thickness swell. In order to make wood-based panels usable for exterior applications, it is necessary to improve their dimensional stability in high relative humidity conditions or during exposure to liquid water (Barnes et al. 2018). To overcome this issue, recent research efforts have focused their energy on increasing OSB dimensional stability by applying different pre-treatments to the wood strands. Figure 2.1 shows the flowchart of the OSB production with the proposed pre-treatment strand step.

Since hemicelluloses are the most hydrophilic polymer in wood due to their highly branched and amorphous structure with more available hydroxyl groups (Weiland and Guyonnet 2003; Hosseinaei et al. 2011; Simpson 1980) extracting hemicelluloses could benefit OSB by reducing thickness swell and water absorption (Okino et al. 2007). There are different techniques available to remove hemicelluloses from wood. In this research was used a hydrothermal treatment (pressurized hot water), which is considered environmental friendly, as it does not utilize any additional chemicals other than water (Garrote et al. 1999). The hydrothermal treatment is an autocatalytic process, where, acidic hydronium ions from hot water aid in the

cleavage of acetyl groups present in hemicelluloses, which subsequently generate organic acids that catalyze hemicelluloses depolymerization (Nabarlatz et al. 2004). As hemicelluloses are amorphous polymers, they are more easily depolymerized than cellulose, which possesses both crystalline and amorphous regions (Sattler et al. 2008). Mild hemicelluloses extraction leaves lignin and cellulose, the structural elements of the wood, intact (Sattler et al. 2008).

Wood strands already have the optimal size to efficiently extract hemicelluloses by hydrothermal process and no additional energy is necessary for wood breakdown. Another advantage of extraction is that it reduces the amount of volatile organic compounds (VOCs) during the manufacturing of the OSB (Paredes 2009). The level of VOCs is restricted due to health hazards and manufacturers currently are monitoring these emissions.

Some investigators have already pursued pressurized hot water extraction on OSB performance but with different tree sources. Paredes et al. (2008) used red maple (Acer rubrum L), which is very different from southern pine in anatomy and chemistry. Maple is only used in a limited OSB industrial capacity in the northern U.S. Since feedstock type appears to be critical (Mirabile et al. 2017) and southern pine (Pinus spp.) is the most used feedstock for OSB in the southern U.S., more research should be performed with pine.

Paredes et al. (2008) found a decrease in strength and internal bond relative to the control after hemicelluloses removal while Hosseinaei et al. (2011) found improvements in modulus of rupture, modulus of elasticity, and internal bond. Therefore, more studies are necessary to better understand what extraction conditions can improve wood composite dimensional stability without any reduction in mechanical properties.

In addition, the study of Hosseinaei was different in that phenol formaldehyde was used and that they pressed for 5 minutes at 200 ºC, while most plants today can press the same

thickness in 3 minutes or less. There is thus a need to test OSB using pine strands but with pMDI coupled with shorter press times.

Hemicelluloses extraction not only could help increase the dimensional stability in OSB but also could benefit the wood composite industry by generating additional revenue for manufacturers. The extraction of hemicelluloses represents an excellent opportunity for the production of chemicals from renewable sources (Mosier et al. 2005). For example, biofuels such as ethanol, butanol, and butanediol can be produced from hemicelluloses as well as other important compounds for the chemical, pharmaceutical, and cosmetics industry such as furfural, lactic acid, xylitol, and polylactic acid. This new source could help meet the increased demand for chemicals currently derived from a petroleum source. This strategy is aligned with the biorefinery concept: to first separate the wood biopolymer (cellulose, hemicelluloses, and lignin) so that high-value products can be obtained (Mihiretu et al. 2017; Il et al. 2017).

This project not only provides important data about the hemicelluloses extraction from wood strands for increasing dimensional stability in OSB but also provides information that can be used for other biomass feedstock and biocomposite materials and will contribute to the production of chemicals using sources other than petroleum. The goal of this study was to remove hemicelluloses from wood strands with pressurized hot water and to test the effect of this pre-treatment on the dimensional stability in humid environmental conditions and mechanical properties of OSB using the ASTM D1037 (ASTM 2012) procedures while using recipes and press times typical of manufacturing.

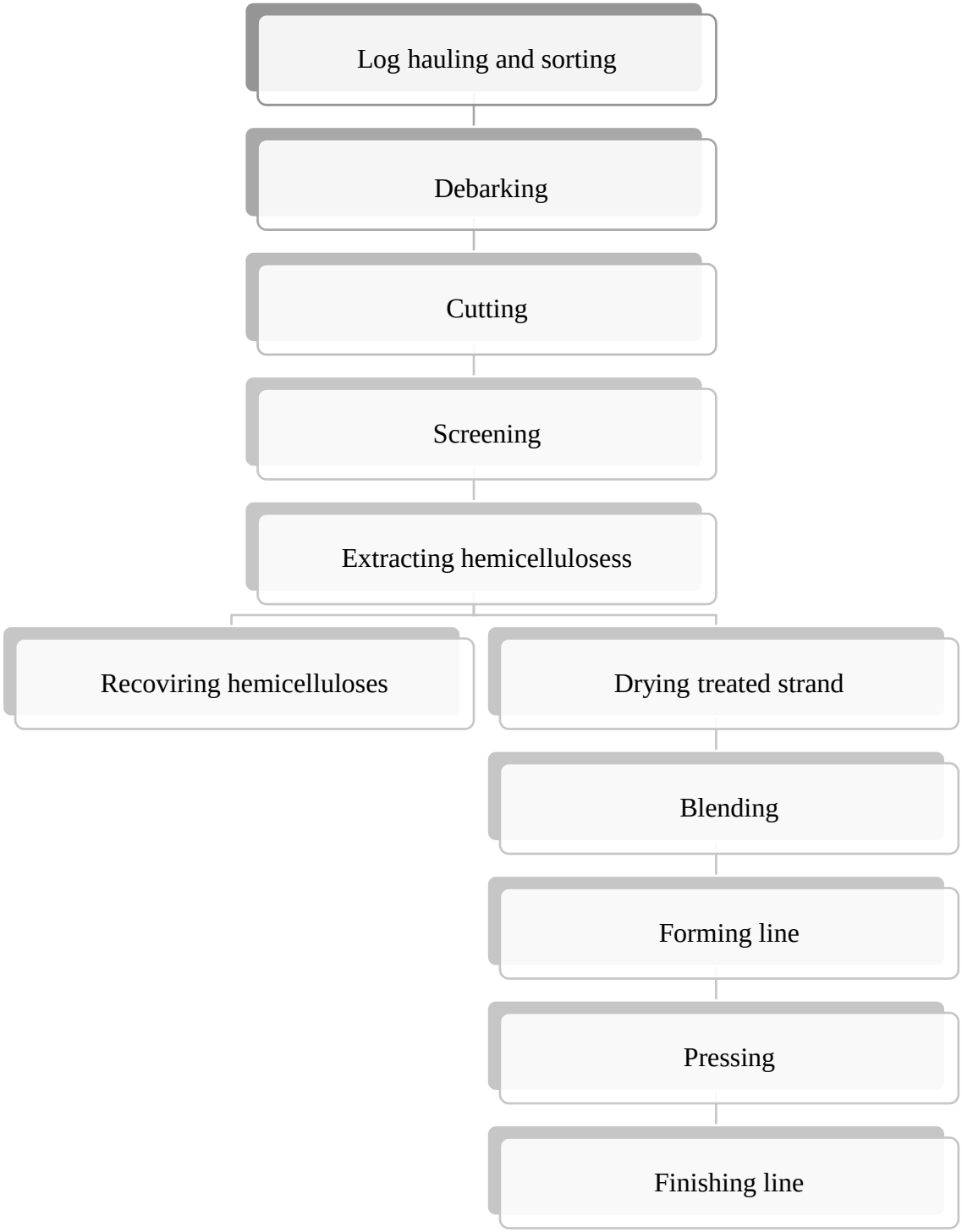

Figure 2.1. Proposed oriented strand boards manufacturing flowchart

2.2. Experimental

2.2.1. Materials and methods

2.2.1.1. Wood strands, resin and wax

Mainly southern yellow pine strands (Pinus spp.) with a 9 % mean moisture content were donated from a local Louisiana Pacific OSB plant. For the preparation of panels, strands retained in a mesh of 1.2 cm were used (largest dimensions were 0.095 cm thickness, 12 cm long and 3.0 cm wide). Commercial pMDI resin (MONDUR 541- Covestro LLC) and emulsified wax additive (Hexion Inc. Ohio USA) were donated from Huber Company. Unless otherwise specified, all the values showed hereinafter on this work are expressed on dry weight basis.

2.2.1.2. Hemicelluloses extraction

Pressurized hot water has been used for extracting hemicelluloses. The most important parameters during the process of hemicelluloses extraction are temperature and time. Temperatures below 120 ºC decrease the amount of hemicelluloses that can be extracted (Sattler 2008), while temperatures above 160 ºC can reduce the grade of polymerization in cellulose (Yu and Wu 2010). Previous work has found high amounts of glucose and cellobiose in the hydrolyzed liquid at 170 °C– 60 min that was an indication of cellulose decomposition (Hosseinaei et al. 2011; Yu and Wu 2010). Thus, it is necessary to find the optimum condition that allow to extract high amounts of hemicelluloses without degrading cellulose. If cellulose is degraded, then the mechanical properties in OSB are likely to decrease. The technique of pressurized hot water extraction can be modeled according to the following equation (Overend and Chornet 1987)

$$S0 = \log \{\exp [(T - 100)/14.75] t\} \quad (2.1)$$

where S0: severity factor, T is the temperature of the treatment (°C), and t is the residence time in minutes. It is possible to achieve the same severity factor at different temperatures by varying times.

This work tested three different temperatures; 120, 140 and 160 °C, and the time was the same for each treatment; 45 min. Hemicelluloses were extracted from 575 g of wood strands (Figure 2.2.a.) using a 6.5 l Parr reactor as shown Figure 2.2.b. (liquor to wood ratio: 1:10). The initial pH of the water was 7.8. The reactor was controlled with a Parr model 4842 controller. The heating temperature ramp was 3 °C/min and the cooling temperature ramp was 8 °C/min. Cooling was done by circulating water through a cooling jacket inside the reactor. The reactor was opened when the temperature was 60 °C and the wood strands were separated from the liquid which was used to measurement the pH. Wood strands were washed with 2 liters of tap water to remove deposited compounds. Then, the washed strands were dried in a ventilated room until a moisture content of approximately 9 % was achieved. Figure 2.2.c shows the treated strands. Strand samples were randomly selected for chemical characterization using High Performance Liquid Chromatography (HPLC).

The percentage of extracted material was calculated by the difference of dry weight before and after extraction according to the following equation:

$$\%\ \text{Extracted Material} = 100 - \frac{\text{g dry strands after extraction} * 100}{\text{g dry strands}\quad \text{before extraction}} \qquad (2.2)$$

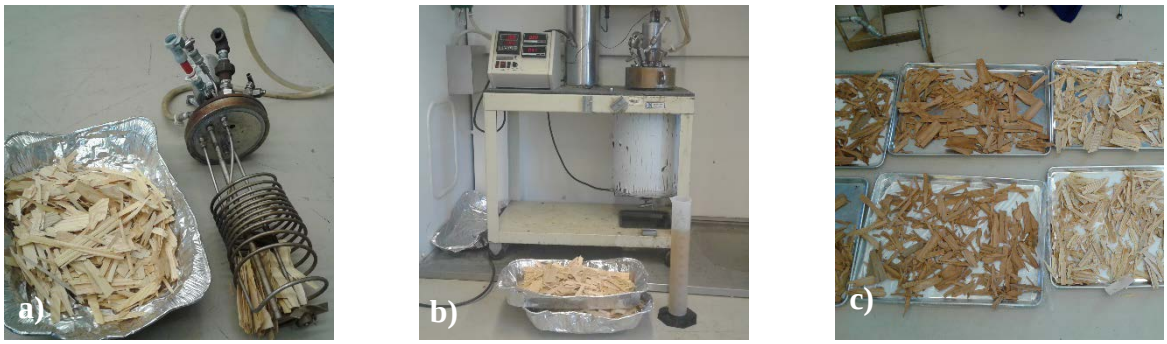

Figure 2.2. a) Untreated wood strands b) Par reactor c) Treated strands

2.2.1.3. Equilibrium moisture content

Equilibrium moisture content was determined by equilibrating strands for 28 days in a closed vessel at 20 ± 2 °C. Each vessel contained different saturated salt solutions to create different relative humidity (RH) environments (Wexler and Hasegawa 1954; Greenspan 1976). Lithium chloride (11.3 % RH), potassium hydroxide (16.7 % RH) magnesium chloride (33.1 % RH), potassium carbonate (43.2 % RH), magnesium nitrate (54.4 % RH), sodium nitrate (75.4 % RH), potassium chloride (85.1 % RH), and potassium sulfate (97.6 % RH) were used in this work. The equilibrium moisture content was calculated with the following equation:

$$\text{Equilibrium moisture content} = \frac{\text{ME -MOD}}{\text{MOD}} * 100 \qquad (2.3)$$

Where: ME is the mass of the sample in equilibrium at the conditioning chamber and MOD is the oven-dried mass of the sample.

2.2.1.4. OSB manufacturing

OSB samples with dimensions of 43 cm × 43 cm were manufactured using the extracted strands as described above, whereas non-extracted strands were used for preparing the control

OSB. In total, eight panels were produced; two panels for each pre-treatment and two for the control. The resin pMDI loading was 2 % dry wt. /dry total board wt. and the emulsified wax was 1 % dry wt. /dry total board wt. A sufficient amount of strands for the production of a single OSB was placed in a concrete mixer and covered with a vinyl covering to reduce spray drift (Figure 2.3.a.). The pMDI and emulsified wax were sprayed using a gravity feed HVLP spray gun (HUSKY model # H4840GHVSG) while the strands were tumbled in the concrete mixer. Panels were hand-formed transferring strands to a forming box placed on a metal sheet and distributed uniformly in the box (Figure 2.3.b.). The forming box was removed, and another metal plate was then placed on the strands mat. Since pMDI reacts with metal of the press, aluminum foil was placed underneath the formed wood strands. The formed mat was then pressed with a Wabash hydraulic press (model 50-24-2TM) (Figure 2.3.c.) under the following conditions: press time 3 min (this time include the interval to close the press and target the desired pressure), temperature 220 °C, and a pressure of 1.6 MPa. Two press stops of 1.1 cm were used on either side of the pressed strands as guides to control the targeted thickness of the panel.

Figure 2.3. a) laboratory blending step b) laboratory forming line c) laboratory pressing step

2.2.1.5. Mechanical and physical properties measurements

For testing of physical and mechanical properties, four samples of dimension 26.7 cm × 7.6 cm and six samples of dimension 5.1 cm × 5.1 cm were obtained from each panel. Half of the larger sized samples were used to measure the modulus of elasticity (MOE-d), and modulus of rupture (MOR-d) in dry conditions. The other half was used to measure water absorption capacity, thickness swell as well as modulus of elasticity (MOE-w) and modulus of rupture (MOR-w) after 24 hours under water submersion. The smaller sized samples were used to measure the internal bond strength. Tests were measured according to American Society for Testing and Materials (ASTM 2012).

To measure water absorption, thickness swelling, MOE-w and MOR-w, the samples were immersed in tap water for 24 hours and special care was taken to prevent samples from floating to the top. A wire netting and weights were used to fully submerge the samples in water. For each sample, the thickness was measured in four pre-market and equally spaced points, at the midpoint of each side, and 2 cm from the edge. Thickness and weight measurements were taken before and after soaking. Samples were allowed to drain on a rack for 10 minutes after the soak before wet measurements were taken. From the measurements, thickness swelling, and water absorption were calculated. Thickness swelling percentage was determined according to equation 2.4 while water absorption percentage was determined according to equation 2.5

$$\%\text{Thickness swelling} = \frac{t_2}{t_1} * 100 - 100 \qquad (2.4)$$

Where t_2 is the average thickness of the 4 point measurement after 24 hours of soaking, and t_1 is the average thickness of the 4 point measurement before 24 hours of soaking.

$$\%\text{Water absorption} = \frac{\text{Final weight- Initial weight}}{\text{Initial weight}} * 100 \quad (2.5)$$

Panel density was determined through the mean density of specimens of all the tests previously mentioned. MTS universal testing machine Zwich/Roell Z010 was used for measuring the mechanical properties of the OSB.

2.2.1.6. Statistical analysis

Analysis of variance ($p < 0.05$) and Fisher's Least Significant Difference (LSD) test were conducted with Statistical Analysis System software (SAS 9.2). The correlation between OSB properties and density was investigated and found to be significant. Therefore, an adjustment of the values using analysis of covariance (ANCOVA), in which the density was the covariate factor was carried out.

2.3. Results and discussion

2.3.1. Hemicelluloses extraction

The amount of extracted material, as well as the acidity of the spent liquid with the hydrolyzed hemicelluloses, increased as severity factor increased (Table 2.1). Many researchers have found a relationship between the temperature treatment and the pH of the spent liquid (Figure 2.4) (Grenman et al. 2011; Rangel et al 2016; Sattler et al. 2008; Tjeerdsma and Militz 2005). Hot water cleaves O-acetyl and generates low molecular weight acids such as acetic acid, which not only decreases the pH of the medium but also catalyses breakage of ether linkages in biomass (Mosier et al. 2005).

Table 2.1. Relation between severity factor, % extracted material and pH of the spent liquid.

Treatment	Severity Factor	% Extracted material	pH spent liquid
120 °C	2.24	1.8 (1.15)	4.6 (0.00)
140 °C	2.83	5.5 (0.03)	4.2 (0.05)
160 °C	3.42	14.1(1.21)	3.8 (0.08)

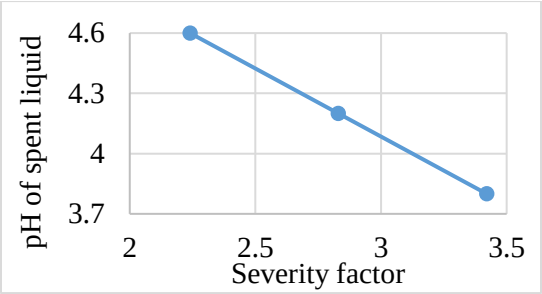

Figure 2.4. Severity factor and their relation with pH of spent liquid

The influence of temperature treatment in the percentage of extracted material is displayed in Figure 2.5. As reported in the literature, the hydrolysis of hemicelluloses is the main reason for the weight loss in wood strands since they are more easily depolymerized than cellulose (Tjeerdsma and Militz 2005). It is also possible for extractives to be a major contributor to weight loss if they are present in large quantities, which is not the case for the material used in this research. The amount of extractive in the material used in this study was only 3.3 %.

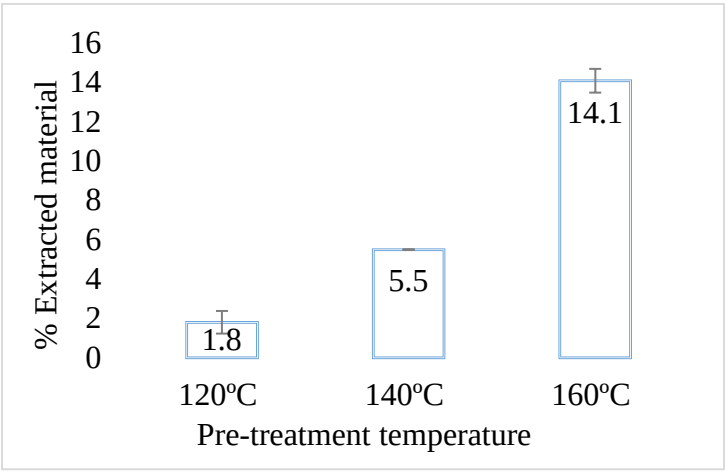

Figure 2.5. Temperature of pre-treatment and their effect in the percentage of extracted material

Table 2.2 shows the percentage of hemicelluloses and cellulose in the control strands and treated strands obtained from the HPLC analysis. At a higher temperature, lower hemicelluloses and higher cellulose percent were present as expected.

Table 2.2. Cellulose and hemicelluloses in control and treated strands

Treatment	% Cellulose	% Hemicelluloses
Control	40.4	17.9
120 °C	43.9	17.7
140 °C	45.5	17.6
160 °C	47.6	14.5

2.3.2. Equilibrium moisture content

The value of equilibrium moisture content was higher for the control than for the pre-treated strands at 160 °C for each relative humidity tested (Figure 2.3). For example, the percent change in mass at 85% RH for the control was 21.8 % while for the pre-treated strands at 160 °C was 18.7%. The same was observed at low relative humidity for example at 11% RH the percent change in mass for the control was 3.56 % while for the pre-treated strands was 2.96 %. The decrease in the equilibrium moisture content was evidence that hydroxyl groups were removed during hemicelluloses extraction. The decreases observed in Figure 2.6 were also in accordance with the improved dimensional stability that was observed during OSB testing (reported shortly).

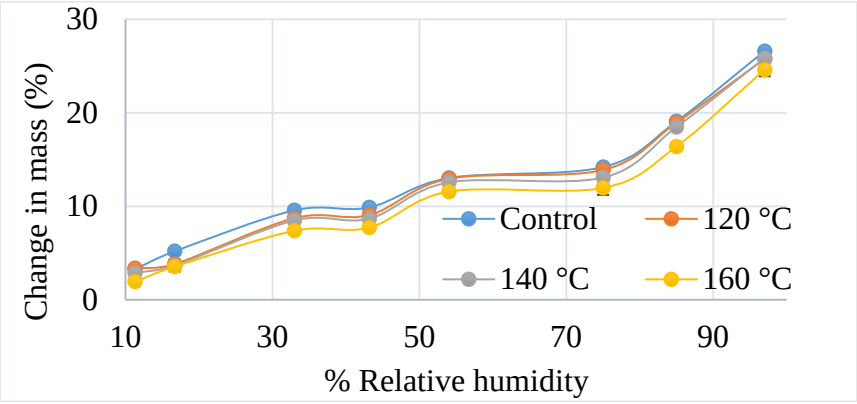

Figure 2.6. Isotherm of the control and pre-treated strands

2.3.3. Mechanical and physical properties measurements

According to the results, the density of the prepared OSB ranged from 0.62 to 0.8 g/cm^3 and the average thickness was in the range of 12.1 to 13.4 mm. The source of the thickness variation was attributable to increased temperatures in which the density and thickness increased and decreased respectively. These results demonstrated that hemicelluloses removal through hydrothermal treatment could help to enhance the compaction of OSB during formation.

Table 2.3 shows the MOE-d, MOR-d, and internal bond strength mean values. For these properties the p-value in the ANCOVA test was bigger than 0.05, indicating that there was not a statistically significant effect at the 95.0 % confidence level between treatment. On the other hand, for the properties of thickness swelling, water absorption, MOE-w, and MOR-w, the p-value was smaller than 0.05, indicating that there was a significate difference between treatment. For these last four properties a Fisher's Least Significant Difference (LSD) test was run. Table 2.4 shows the result of LSD as well as the mean of these properties.

Table 2.3. Mean value of MOE-d, MOR-d, and internal bond strength OSB property under dry conditions.

Treatment	MOE-d (MPa)	MOR-d (MPa)	Internal bond strength (N/mm^2)
Control	3818 ± 485	25.2 ± 4.6	0.44 ± 0.06
120 ºC	3766 ± 439	27.4 ± 4.2	0.46 ± 0.04
140 ºC	3278 ± 434	23.4 ± 4.1	0.45 ± 0.06
160 ºC	3864 ± 637	26.9 ± 6.1	0.51 ± 0.09

Table 2.4. Mean value and result of Fisher's Least Significant Difference (LSD) test of thickness swelling, water absorption, MOE-w, MOR-w OSB property in wet conditions.

Treatment	Thickness swelling (%)	Water absorption (%)	MOE-w (MPa)	MOR-w (MPa)
Control	28.3 ± 2.3 a	63.1 ± 4.3 a	894 ± 323 c	8.4 ± 5.0 c
120 ºC	22.2 ± 2.3 b	42.7 ± 4.3 b	1139 ± 246 b-c	11.1 ± 3.8 b-c
140 ºC	18.4 ± 2.3 c	39.0 ± 4.3 b – c	1407 ± 246 b-a	14.8 ± 3.8 b-a
160 ºC	14.6 ± 2.3 d	34.1 ± 4.4 c	1751 ± 281 a	18.4 ± 4.33 a

The same letter in a column indicates that there is no statistical difference ($p > 0.05$) between the specimens according to Fisher's Least Significant Difference (LSD) test.

For the data set obtained in wet conditions, the benefits of the pre-treatments were rather clear, and a significant improvement in dimensional stability (thickness swelling and water absorption) with increased temperature pre-treatment were observed. In addition, increased temperatures increased the MOE-w and MOR-w mean values. The OSB prepared after the pre-treatment of wood strands at 160 °C showed the best performance for these four properties, with an improvement of around 50 % compared to the control.

Figure 2.7 shows the benefits of the hemicelluloses extraction on physical properties. A significant decrease in thickness swelling and water absorption when the temperature of the pre-treatment increased were observed.

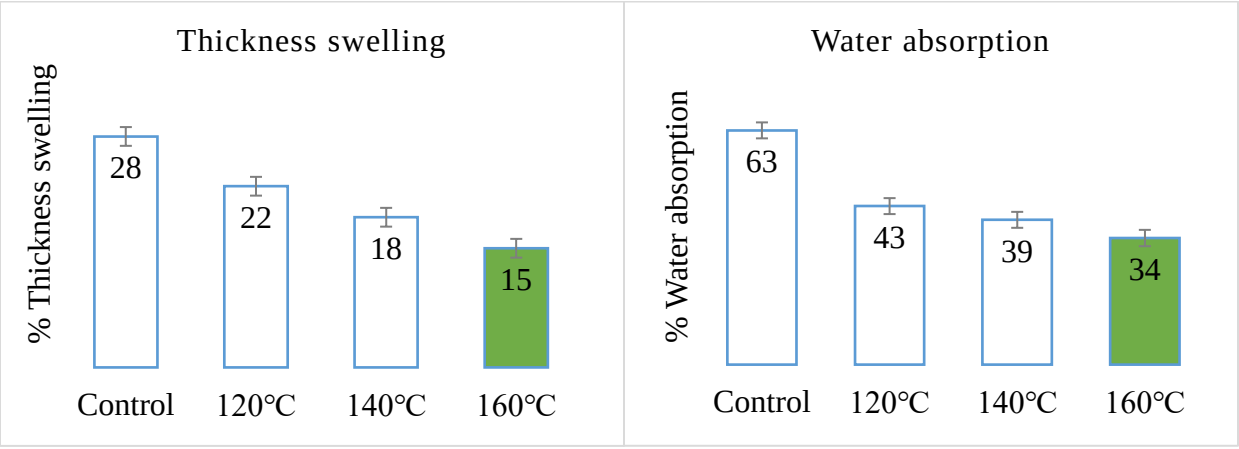

Figure 2.7. Dimensional stability of the control and pre-treated OSB.

The positive impact on the dimensional stability of the composite can be attributed to the selective removal of hemicelluloses (Hosseinaei et al. 2011). The removal of hemicelluloses allowed for the production of compact OSB in this study, and was in agreement with Pelaez-Samaniego et al (2013). Apparently, with lower porosity, the tendency of moisture migration into the wood is reduced during short-term exposure (Ayrilmiş et al. 2017). Furthermore, the removal of these heteropolysaccharides decreased the available carboxyl- and hydroxyl groups which are responsible for water uptake, making the matrix less hydrophilic (Weiland and Guyonnet 2003). Also possibly, the pre-treatment at higher temperatures allows lignin to become fluid, moving out through the cell wall matrix and the lignin redepositing on the surface once the temperature is decreased (Donohoe et al. 2008). Thus, the lignin-enriched wood strands surface become more hydrophobic (Axelsson et al. 2012).

Figure 2.8 shows the benefits of hemicelluloses extraction in mechanical properties. A significant increment in MOE-w and MOR-w mean values when the temperature of the pretreatment increased was observed.

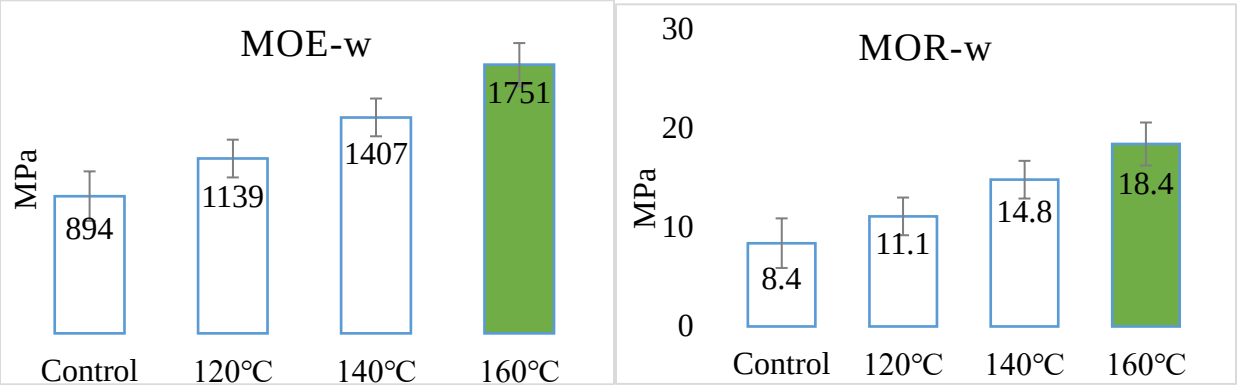

Figure 2.8. Mechanical properties in wet conditions of the control and pre-treated OSB.

The improvement in the MOE-w and MOR-w mean values can be mainly attributed to the mild extraction conditions. Mild extractions that do not destroy the long cellulose chain while allowing for the removal the amorphous and branched hemicelluloses results in a more compact OSB composite.

2.4. Conclusions

The removal of hemicelluloses from wood strands with pressurized hot water improved the dimensional stability of OSB. This was attributed to less available hydroxyl groups associated to the presence of hemicelluloses. The percentage of extracted material increased as reaction temperature increased in the range of temperatures studied. At 120 °C, the percent of hemicelluloses extracted was reduced and its impact on final OSB properties was insignificant. Pre-treatment at 160 °C resulted in the maximum amount of hemicelluloses extraction. At this pre-treatment temperature, OSB had the best dimensional stability. In hindsight, perhaps higher temperatures are possible before mechanical properties begin to degrade, and more studies should be performed in order to explore this possibility.

MOE-d, MOR-d, and internal bond strength properties were not affected by the hemicelluloses extraction. In other word, OSB produced with treated strand and non-treated strands had almost the same value for these properties.

References

ASTM. (2012). D1037 Standard Test Methods for Evaluating Properties of Wood-Base Fiber and Particle Panel Materials. American Society for Testing and Materials, West Conshohocken, PA.

Axelsson, L., Franzén, M., Ostwald, M., Berndes, G., Lakshmi, G., and Ravindranath, N. (2012). Jatropha cultivation in southern India: Assessing farmers' experiences. Biofuels, Bioproducts and Biorefining. 6(3):246–256.

Ayrilmiş, N., Kwon, J., and Han, T. (2017). Effect of wood chip size on hemicellulose extraction andtechnological properties of flakeboard. Turk J Agric For. 41:331–337.

Barnes, H., Aro, M., and Rowlen, A. (2018). Thermally Modified Engineered Wood Products Durability. Forest Products Journal. 68(2).

Cheng, Q., Zhou, C., Jiang, W., Zhao, X., Via, B., and Wan, H. (2018). Mechanical and Physical Properties of Oriented Strand Board Exposed to High Temperature and Relative Humidity and Coupled with Near-Infrared Reflectance Modeling. Forest Products Journal. 68(1):78-85.

Donohoe, B., Decker, S., Tucker, M., Himmel, M., and Vinzant, T. (2008). Visualizing lignin coalescence and migration through maize cell walls following thermochemical pretreatment. Biotechnology and Bioengineering. 101(5):913–925.

Garrote, G., Domínguez, H., and Parajó, J. (1999). Mild autohydrolysis: an environmentally friendly technology for xylooligosaccharide production from wood. Chem Technol Biotechnol. 74(11):1101–1109.

Greenspan, L. (1976). Humidity Fixed Points of Binary Saturated Aqueous Solutions. Journal of Research of the National Bureau of Standards, 81A(1).

Grenman, H., Eranen, K., Krogell, J., Willfor, S., Salmi, T., and Murzin, D. (2011). Kinetics of aqueous extraction of hemicelluloses from spruce in an intensified reactor system. Ind. Eng. Chem. Res. 50(7):3818–3828.

Hosseinaei, O., Wang, S., Rials, T. G., Xing, C., and Zhang, Y. (2011). Effects of decreasing carbohydrate content on properties of wood strands. Cellulose. 18(3):841–850.

Il, W., Jin, H., Ju, S., and Keun, K. (2017). Thermo-mechanical fractionation of yellow poplar sawdust with a low reaction severity using continuous twin screw-driven reactor for high hemicellulosic sugar recovery. Bioresource Technology. 241:63–69.

Lippke, B., and Edmonds, L. (2006). Environmental performance improvement in residential construction: The impact of products, biofuels, and processes. Forest Product Journal. 54(6).

Mihiretu, G., Brodin, M., Chimphango, A., Øyaas, K., Hoff, B., and Görgens, J. (2017). Single-step microwave-assisted hot water extraction of hemicelluloses from selected lignocellulosic materials – A biorefinery approach. Bioresource Technology. 241:669–680.

Mirabile, K. and Zink-Sharp, A. (2017). Fundamental Bonding Properties of Douglas-Fir and Southern Yellow Pine Wood. Forest Products Society. 67(7):435–447.

Mosier, N., Wyman, C., Dale, B., Elander, R., Lee, Y., Holtzapple, M., and Ladisch, M. (2005). Features of promising technologies for pretreatment of lignocellulosic biomass. Bioresource Technology. 96(6):673–686.

Nabarlatz, D., Farriol, X., and Montané, D. (2004). Kinetic modeling of the autohydrolysis of lignocellulosic biomass for the production of hemicellulose-derived oligosaccharides. Ind. Eng. Chem. Res. 43(15):4124–4131.

Okino, E., Teixeira, D., and Del Menezzi, C. (2007). Post-Thermal Treatment of Oriented Strandboard (Osb) Made From Cypress (Cupressus Glauca Lam.). Maderas Ciencia y Tecnología. 9(3):199–210.

Overend, R., and Chornet, E. (1987). Fractionation of lignocellulosics by steam-aqueous pretreatments. Philosophical Transactions of the Royal Society of London. 321:523–536.

Paredes, J. (2009). Influence of hot water extraction on the physical and mechanical behavior of OSB. Masters thesis in the University of Maine, 42 Stodder Hall Orono Maine.

Paredes, J., Jara, R., Heiningen, A. and Shaler, S. (2008). Influence of hot water extraction on the physical and mechanical behavior of OSB. Forest Product Journal. 58(12):56–62.

Paul, W., Ohlmeyer, M., Leithoff, H., Boonstra, M., and Pizzi, A. (2006). Optimising the properties of OSB by a one-step heat pre-treatment process. Holz Als Roh - Und Werkstoff. 64(3):227–234.

Pelaez-Samaniego, M., Yadama, V., Lowell, E., and Espinoza-Herrera, R. (2013). A review of wood thermal pretreatments to improve wood composite properties. Wood science and technology. 47(6):1285–1319.

Rangel, J., Hornus, M., Felissia, F., and Area, M. Hydrothermal treatment of eucalyptus sawdust for a forest biorefinery. Cellulose chem. Technol. 50 (5-6): 521-528

Sattler, C. (2008). Value Prior to Processing of Oriented Strand Board Flakes Through Hot Water Extraction. Masters Theses in the University of Tennessee - Knoxville.

Sattler, C., Labbé, N., Harper, D., Elder, T., and Rials, T. (2008). Effects of hot water extraction on physical and chemical characteristics of oriented strand board (OSB) wood flakes. Clean. 36(8):674–681.

Simpson, W. (1980). Sortpion theories applied to wood. Wood and Fiber, 12(3), 183–195.

Tjeerdsma, B., and Militz, H. (2005). Chemical changes in hydrothermal treated wood: FTIR analysis of combined hydrothermal and dry heat-treated wood. Holz Als Roh - Und Werkstoff. 63(2):102–111.

Weiland, J., and Guyonnet, R. (2003). Study of chemical modifications and fungi degradation of thermally modified wood using DRIFT spectroscopy. Holz Als Roh- Und Werkstoff. 61(3):216–220.

Wexler, A., and Hasegawa, S. (1954). Relative humidity-temperature relationships of some saturated salt solutions in the temperature range 0º to 50 ºC. Journal of Research of the National Bureau of Standards. 53(1):19.

Yu, Y., and Wu, H. (2010). Significant differences in the hydrolysis behavior of amorphous and crystalline portions within microcrystalline cellulose in hot-compressed water. Industrial and Engineering Chemistry Research. 49(8):3902–3909.

Chapter 3

Partial substitution of pMDI with CNF in oriented strand board.

3.1. Introduction

In recent years, the demand for wood composites has increased (Hammett et al. 2002) and as a consequence, the request for wood adhesives has grown. These adhesives are predominantly made from non-renewable resources (Imam et al. 2001); therefore, alternative renewable materials need to be developed to supply the increase in adhesive use. One material that has caught the attention of researchers in the last several years is cellulose nanofibrils (CNF) which is renewable and has a high modulus of elasticity (Benítez et al. 2017; Mi-Jung Cho et al. 2011; Klemm et al. 2011). Partial replacement of pMDI adhesive in wood composites by CNF could reduce the demand for petroleum-based chemicals needed to produce pMDI that is the most common adhesive in OSB panels. The annual production of OSB in the United States is around 20,000,000 m^3/year (Production of Wood-based Panels 2013), which means around 119,000 tons of pMDI are used per year to produce OSB. If 5 % of pMDI were to be replaced by CNF, a resulting decrease in usage of 5,950 tons/year of pMDI would occur.

During the manufacturing of OSB, there are variables that need to be controlled. Therefore, screening the experimental set-ups were necessary to verify the testing methods to properly compare CNF substituted resins with their neat resin counterparts. Proper strand board formation was required to compare the resins and observe the effect of CNF on pMDI. Screening work involved the adjustment of temperature, pressure, density, thickness, uniform distribution of strands across the panel during the formation step and adhesive dispersion. After the

appropriate conditions for the addition of CNF were found, two experiment designs were performed to test the effect of CNF substitution in synthetic wood adhesives. One experimental design was run on OSB panel with density 0.51 g/cm^3 and the second with density 0.60 g/cm^3. The volume of the finished board is held constant. Therefore, density is manipulated by adjusting the total mass of the board.

The goal of this research was to study the alternative of partial replacement of pMDI by unbleached CNF in OSB. Since CNF has a high modulus of elasticity (Auad et al. 2008), the use of this could not only reduce the consumption of pMDI, but it could also reinforce the OSB panel. The behavior of the new blending was analyzed by the measurement of dimensional stability and mechanical properties on OSB panel using ASTM D1037 (ASTM 2012) procedures.

3.2. Experimental set-up

3.2.1. Materials and Methods

3.2.1.1. Wood strands, pMDI, CNF and wax

The pMDI used was MONDUR 541- Covestro LLC. A moisture content of zero was assumed for mixing applications. The emulsified wax used was Hexion Inc. Ohio USA. The solids content was reported as 47 %. Both the pMDI and wax were donated from Huber Company. Southern yellow pine strands were supplied by Norbord, which is an OSB Plant, located in Lanett Alabama. Strands retained in a mesh of 1.2 cm were used for OSB manufacturing. Unbleached CNF with a concentration of 1.9 wt. % was prepared at the Forest Products Laboratory at Auburn University. To obtain the CNF, softwood cellulose KRAFT with Kappa number 20.76 that represents 3.11 % of lignin was refined with Masuko MKZA-10-15J.

3.2.1.2. Adhesive mixing and increasing CNF concentration.

Adhesive mixing was labeled throughout this screening experimental set-up with the amount of CNF substituted in them: dry wt. % CNF/total dry wt. adhesive, for practical reason instead to write, for example, 2 dry wt. % CNF/total dry wt. adhesive is written as 2 % CNF. Adhesive refers in this work as the mix of CNF and pMDI. Different concentrations of mixture with CNF in pMDI and CNF in wax were prepared. Mixtures of 2.6 % CNF (1.9 wt. % CNF) in pMDI, 2.6 and 5 % CNF (1.9 wt. % CNF) in wax, and 2.6 % CNF (7 wt. % CNF. CNF was concentrated by a rote evaporator) in wax were prepared. In addition, a mixture of freeze-drying CNF in wax was tested. Freeze-drying CNF was ground with a mortar and enough amount of it was added in wax to get a solution of 2.6 % CNF in wax. In each case, CNF was added to the wax and mixed by hand and then by a bath sonicator for 30 min.

3.2.1.3. OSB manufacturing

Panels with different densities, % adhesive, % CNF, and temperature of pressing were tested (Table 3.1). Sufficient amount of strands depending on the density for the production of a single OSB were placed in a concrete mixer and covered with a vinyl covering to reduce spray drift. The pMDI, CNF, and emulsified wax were sprayed separately using a gravity feed HVLP spray gun while the strands were tumbled in the concrete mixer. The wax was applied at 1 % dry wt./dry total board wt. while the amount of pMDI and CNF were applied according to Table 3.1 Panels were hand-formed by transferring strands to a forming box placed on a metal sheet and distributed uniformly throughout the box. The forming box was removed, and another metal plate was then placed on the strand mat. Since pMDI reacts with metal of the press, aluminum foil was placed underneath the formed wood strands. Two press stops of 11 mm were used on either side of the pressed strands as guides to control the targeted thickness of the panel. The

formed mat was then pressed with a Wabash hydraulic press (model 50-24-2TM) under the following conditions: press time 3 min and pressure 2.1 MPa.

Table 3.1. Panel density, temperature of pressing, amount pMDI and CNF.

Trial	Density (g/cm^3)	Temperature of pressing (°C)	For 100 g of dry wood strands			Percentage based on total OSB		CNF respect to adhesive (%)
			pMDI (g)	CNF-dry based (g)	CNF-water (g)	Adhesive[2] (%)	CNF (%)	
1	0.53	210 ± 10	6.1	0.3	17	6.0	0.3	4.7
2	0.58	240 ± 10	6.2	0.2	9	6.0	0.2	3.1
3	0.58	210 ± 10	6.2	0.2	9	6.0	0.2	3.1
4	0.61	210 ± 10	4.3	0.2	12	4.3	0.2	4.4
5	0.61	210 ± 10	1.9	0.1	5	2.0	0.1	5.0
6[1]	0.64	210 ± 10	4.2	-	-	4.0	-	-

[1] Trial 6, instead CNF it was sprayed 5 g of water per 100 g dry wood.
[2] Adhesive refers the sum of pMDI and CNF

3.2.2. Results and discussion

3.2.2.1. Adhesive mixing and increasing CNF concentration

The mixture of CNF with pMDI (Figure 3.1.a) was not homogenous and after one hour, a lot of bubbles were observed from the mixture. As it was explained in section 1.6, the bubbles are attributed to carbon dioxide gas that is one of the products formed during the reaction between isocyanate group from pMDI and water (Fred et al. 1996; Leventis et al. 2010; Niyogi 1999; Xiaobin et al. 2007) from the nanocellulose suspension. The mixture of 2.6 % CNF in wax was homogenous to the naked eye (Figure 3.1.b). Figure 3.1.c shows the CNF 7 wt. % which was not fluid. At 25 ± 5 ºC the 2.6 % CNF in wax with CNF 7 wt. % as well with CNF wt. 1.9 clogged the gun that was used for OSB production when the mixture was being sprayed (Figure 3.1.d). The mixture of 2.6 % freeze-drying CNF in wax was not homogenous; it was not possible to dissolve the freeze-dried CNF, which looks like a carton.

Figure 3.1. a) CNF with pMDI, b) CNF with wax, c) CNF 7 wt. %, d) Not fluid mixture of CNF in wax

It is important to get a homogeneous mixture and uniformly spray the adhesives and additives during OSB production and without clogging; because a flaw in the adhesive-bonded wood can be produced by a discontinuity, such as a void, or an abrupt change in material properties (Frihart 2005). Since spraying components together was difficult and the viscosity of the mixture increased as the time passed, it was decided to spray them separately. High viscosity not only could clog the spray system but also reduce the wetting capability and penetration of the adhesive (Kamke 2007). The penetration of adhesive below the wood surface is important to improve bonding forces. Greater penetration is associated with more surface contact between the wood substance and the adhesive (Pizzi 1994; Kamke 2007). Not only was spraying a mixture of CNF-wax difficult, but it was also problematic to spray the CNF 2 wt. % by itself. Both approaches have clogged the gun with agglomeration of nanocellulose (Figure 3.2.a). To reduce this problem, the 1.4 mm pin stream nozzle was replaced by a 1.8 mm pin stream nozzle and an extra line of compressed air was used to help nanocellulose spray out of the gun (Figure 3.2.b).

Although CNF has nanoscale diameter, the length is in the order of microns (Zimmermann et al. 2010; Klemm et al. 2011) and it could reduce the penetration of pMDI in the lumen of the wood that has microns dimension (Manwiller 1972; Mäkinen et al. 2002).

Therefore, it was decided to first spray pMDI, then CNF, and lastly wax in order to negate the reduction of penetration.

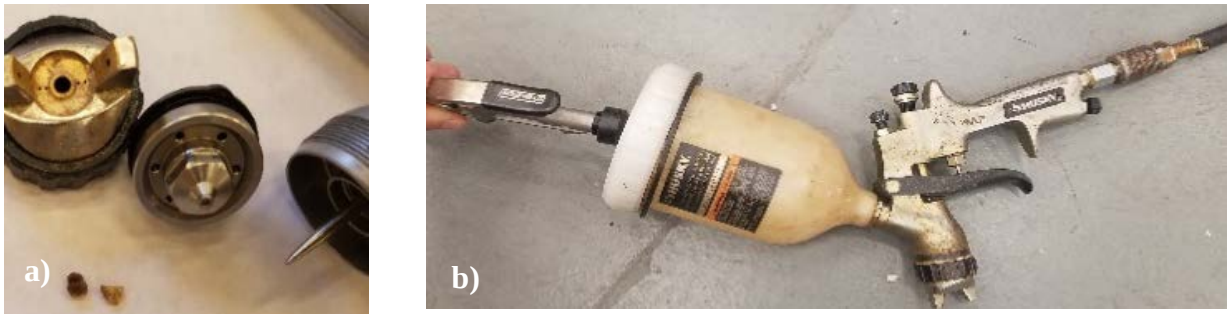

Figure 3.2. a) Pin stream Nozzle and CNF aagglomeration b) Laboratory system spray gun with two lines of compressed air.

3.2.2.2. Delamination problem in OSB

OSB panels 2, 4, and 6 produced according to Table 3.1 presented delamination problem (Figure 3.3) while the rest of the samples did not. As it was mentioned before, the reaction between the isocyanate group and water produces CO_2, and this component and the water from CNF can cause the delamination problem. During the pressing step, temperatures higher than 180 °C was used to cure the adhesive. While in this condition water and CO_2 are in a gas state which causes high internal pressure within the composite and when the steam is not able to escape fast enough it results in heightened pressure (as a consequence, delamination). OSB 2 had a delamination problem while OSB 3 did not have, and the only difference between them was that OSB 2 was pressed at 30 °C higher than OSB 3. We came to the conclusion that temperature plays an important role in delamination issues. At higher temperatures, the pressure of water and CO_2 are higher causing more delamination problems. In OSB 6, water was added instead of CNF, and it presented a delamination problem indicating that the water in CNF was responsible for the problem and not the CNF itself. The differences between OSB 3 and 4 were their density, percentage of CNF and adhesive. OSB 4 had a higher density and percentage of CNF presenting

a delamination problem. OSB 4 and 5 had the same density, but the amount of CNF in OSB 5 was less and it did not present a delamination problem. OSB 1 had the lowest density and high percentage of CNF and it did not present a delamination problem. Therefore, these examples showed that density and temperature were the main factors in the delamination issues. Furthermore, the results showed that low-density samples did not present a delamination problem indicating that the steam was able to escape from the composite because there were more free channels.

Figure 3.3. Delamination problem in panel

3.2.3. Preliminary conclusion

Working with CNF as a partial replacement of non-renewable adhesive presents the challenge of dealing with delamination issues. Water that is contained in CNF and CO_2 from the reaction between isocyanate group and water can cause, at high temperatures, a lot of steam; which generates high internal pressure in panels, resulting in a delamination problem. The alternative of reducing the water in CNF and then spray had the inconvenience of high viscosity. Nanocellulose with a concentration higher than 3 % was not fluid enough to move out of the spray gun's nozzle and this resulted in clogging or blockage of the gun. Therefore, we proposed to produce low-density panels, which are less compact, where water can escape from the increased number of free voids in the panel. Moreover, we proposed to work with a pressing temperature lower than 210 ± 10 °C. With respect to the spraying system, it was decided to separately spray pMDI, CNF, and wax because it was not easy to get a homogenous solution in most of the cases.

3.3. Experimental design

3.3.1. Materials and Methods

3.3.1.1. Wood strands, pMDI, CNF and wax

The pMDI used was MONDUR 541- Covestro LLC. A moisture content of zero was assumed for mixing applications. The emulsified wax used was Hexion Inc. Ohio USA. The solids content was reported as 47 %. Both the pMDI and wax were donated from Huber Company. Norbord OSB Company, in Lanett Alabama, supplied southern yellow pine strands. Strands retained in a mesh of 1.2 cm were used for OSB manufacturing. Unbleached CNF with a concentration of 1.9 wt. % was prepared at the Forest Products Laboratory at Auburn University. To obtain the CNF, softwood cellulose KRAFT with Kappa number 20.76 that represents 3.11% of lignin was refined with Masuko MKZA-10-15J.

3.3.1.2. Experimental design and OSB manufacturing

Two experimental designs with a low and high target density were executed. The density in the first experimental design was 0.51 g/cm^3 and in the second, it was 0.60 g/cm^3. Each experimental design involved two factors: adhesive (pMDI and CNF) and CNF and three levels for each factor (Table 3.2).

Table 3.2. Experimental design with adhesive and CNF as factors

	Factors (real values)		Factors (coded values)	
Trial	(%) adhesive[1] based on total OSB	(%) CNF respect to adhesive	(%) adhesive based on total OSB	(%) CNF respect to adhesive
1		0		-1
2	2.7	3	-1	0
3		6		1
4		0		-1
5	4.4	3	0	0
6		6		1
7		0		-1
8	6.2	3	1	0
9		6		1

[1]Adhesive refers to the sum of pMDI and CNF

Sufficient amounts of strands for the production of a single OSB were placed in a concrete mixer and covered with a vinyl covering to reduce spray drift. The pMDI, CNF and emulsified wax were sprayed separately using a gravity feed HVLP spray gun while the strands were tumbled in the concrete mixer. The wax was applied at 1 % dry wt./dry total board wt. while the amount of pMDI and CNF were applied according to Table 3.3. Panels were hand-formed transferring strands to a forming box placed on a metal sheet and distributed uniformly in the box. The forming box was removed, and another metal plate is then placed on the strands mat. Since pMDI reacts with metal of the press, aluminum foil was placed underneath the formed wood strands. Two press stops of 11 mm were used on either side of the pressed strands as guides to control the targeted thickness of the panel. The formed mat was then pressed with a Wabash hydraulic press (model 50-24-2TM) under the following conditions: press time 3.5 min, temperature 180-220 °C, and pressure 2.1 MPa.

Table 3.3. OSB composition of the experimental design at low and high target density

Trial	Density (g/cm^3)	For 100 g of dry wood strands			Percentage based on total OSB (dry wood, pMDI, and CNF)		CNF respect to adhesive (%)
		pMDI (g)	CNF-dry based (g)	CNF-water (g)	Adhesive (%)	CNF (%)	
1	0.51	2.8	0.0	0	2.7	0.0	0
2	0.51	2.7	0.1	5	2.7	0.1	3
3	0.51	2.5	0.2	12	2.7	0.2	6
4	0.51	4.6	0.0	0	4.4	0.0	0
5	0.51	4.5	0.1	7	4.4	0.1	3
6	0.51	4.4	0.3	15	4.4	0.3	6
7	0.51	6.6	0.0	0	6.2	0.0	0
8	0.51	6.4	0.2	11	6.2	0.2	3
9	0.51	6.2	0.4	21	6.2	0.4	6
1	0.60	2.8	0.0	0	2.7	0.1	0
2	0.60	2.7	0.1	5	2.7	0.2	3
3	0.60	2.5	0.2	12	2.7	0.0	6
4	0.60	4.6	0.0	0	4.4	0.1	0
5	0.60	4.5	0.1	7	4.4	0.3	3
6	0.60	4.4	0.3	15	4.4	0.0	6
7	0.60	6.6	0.0	0	6.2	0.0	0
8	0.60	6.4	0.2	11	6.2	0.2	3
9	0.60	6.2	0.4	21	6.2	0.4	6

[1]Adhesive refers the sum of pMDI and CNF

3.3.1.3. Mechanical and physical properties measurements

Samples of dimension 27.2 cm × 7.6 cm were used to measure modulus of elasticity (MOE-d) and modulus of rupture (MOR-d) in dry conditions. Modulus of elasticity (MOE-w), modulus of rupture (MOR-w), absorption capacity and thickness swelling were measured after the samples were submerged under water for 24 hours. Each property was measured in quadruplicate. Samples of dimension 5.1 cm × 5.1 cm were used to measure internal bonding. The procedures of these tests were explained in section 1.4. The static bending (modulus of

elasticity and modulus of rupture) and internal bond strength were measured with MTS universal testing machine Zwich/Roell Z010.

3.3.1.4. Statistical analysis

Experimental design analysis was run to identify the effect of adhesive and CNF at low and high density on MOR-d, MOE-d, thickness swelling, water absorption, MOR-w, MOE-w, and internal bonding OSB properties. In addition, since density was not possible to maintain at the target value and it varies through the OSB panel around the desired value it was decided to run a multiple linear regression in which density was included as an independent factor. Variables were determined to be significant at $\alpha = 0.05$ level. The R^2 was reported to estimate the percentage of variation that the independent variables contributed to each property. The data was analyzed using Statgraphics Centurion Version 18.1.06 software

3.3.2. Results and discussion

3.3.2.1 Analysis of the experimental design

Table 3.4 displays the average and standard deviation of samples for each property that was measurement. Table 3.5 summary the p-values of the adhesive and CNF for MOE-d, MOR-d, MOE-w MOR-w, thickness swelling, water absorption, and internal bonding properties of the experimental design. Figure 3.5 displays the effect of adhesive and CNF in these properties at low and high-density panel.

Table 3.4. Average and standard deviation of samples for thickness swelling, water absorption, MOE-d, MOR-d. MOE-w, MOR-w and internal bond property

		Thickness swelling (%)		Water absorption (%)		MOE-w (Mpa)		MOR-w (Mpa)		MOE-d (Mpa)		MOR-d (Mpa)		Internal bond (N/mm2)	
Adhesive	CNF	Aver.	STDEV	Aver.	STDEV	Aver.	STDEV	Aver.	STDEV	Aver.	STDEV	Aver.	STDEV	Aver.	STDEV
Low density															
2.7	0	22.8	2.3	63.6	7.0	944	270	6.4	2.4	2630	531	14.4	3.7	0.31	0.02
4.4	0	17.5	1.4	53.6	3.5	1128	267	7.5	1.2	2858	482	16.4	3.0	0.41	0.06
6.2	0	15.0	0.8	46.6	6.7	1445	419	10.3	3.0	2925	651	17.1	6.2	0.73	0.07
2.7	3	25.6	2.6	69.1	6.3	836	157	6.5	1.7	2908	230	17.3	4.1	0.34	0.09
4.4	3	16.6	0.7	57.5	4.0	1344	512	10.3	4.6	2643	523	17.2	4.9	0.43	0.03
6.2	3	15.6	0.8	51.3	1.7	1459	465	10.5	2.9	3315	957	20.3	9.3	0.45	0.09
2.7	6	26.1	1.8	83.9	24.9	816	223	6.5	1.3	3470	473	21.7	2.3	0.26	0.03
4.4	6	18.2	2.0	59.8	3.9	1252	444	8.6	4.0	3668	875	23.1	8.8	0.38	0.06
6.2	6	14.3	1.8	51.4	6.4	1843	461	12.6	4.1	3175	197	17.5	2.0	0.35	0.08
High density															
2.7	0	25.9	0.7	43.1	4.6	749	128	5.2	1.3	3040	569	17.3	1.1	0.18	0.02
4.4	0	16.8	1.1	31.3	3.1	1463	244	11.8	2.9	3818	1141	23.0	8.7	0.23	0.03
6.2	0	14.4	2.2	31.6	3.4	1246	317	10.4	4.5	2843	624	19.1	3.5	0.40	0.09
2.7	3	23.3	0.8	45.3	1.9	751	102	5.6	1.1	3160	506	18.7	6.9	0.20	0.06
4.4	3	14.5	1.9	37.0	6.4	1338	332	11.1	3.7	3485	851	23.2	5.2	0.34	0.05
6.2	3	13.2	1.0	32.8	4.8	1595	140	12.3	2.3	3815	613	24.7	7.6	0.39	0.09
2.7	6	23.6	1.0	50.6	4.9	765	16	4.6	1.0	3465	211	20.8	4.8	0.26	0.07
4.4	6	14.2	2.4	34.9	7.8	1658	257	11.2	3.4	3383	492	19.5	3.1	0.17	0.07
6.2	6	13.0	4.1	35.2	11.6	1508	316	9.5	2.2	3513	411	24.1	4.6	0.21	0.04

The analysis showed that the effect of CNF had the same tendency at low and high density, but the relevance of this effect was not the same. For instance, if we compared the effect of CNF on the MOE-d at low and high density (Figure 3.5), in both cases, the addition of CNF had the tendency to increase the value of this property, but only in the case of low density, the p-value displayed a statistically significant effect at the 95.0 % confidence level. The positive effect of CNF could be due to the high modulus of elasticity of the CNF (Spence et al. 2010; D Klemm et al. 2011; Moon et al. 2011). Maybe the reaction between isocyanate groups from the pMDI with the hydroxyl groups of the CNF help to fill the networking adhesive and reduce the discontinuity in the adhesive-bonded wood. CNF also had a significant positive effect on MOR-d and a negative effect on internal bonding at low density. The reduction of the internal bonding

could be due to the extra water added to the panel by the CNF substitution and CO_2 from the reaction between isocyanate group and water. At high temperatures, water and CO_2 can generate high internal pressure in panels causing the spring back and consequently a flaw in the adhesive-bonded wood.

At low and high density, the adhesive had a significant effect on thickness swelling, water absorption, MOE-w MOR-w, and internal bonding. In all these properties, the more adhesive, the better the properties were. It can be explained by the bonding strength of pMDI. The –NCO groups from pMDI react with the –OH groups of the cellulose and forms as "covalent bonds" in the form of urethane linkages (Nugroho and Ando 2000). However, it is not desirable to increase the amount of pMDI because it is expensive and not renewable.

Table 3.5. P-values for adhesive and CNF factors at low and high target density from the analysis of the experimental design.

Property	Independent variable	Low density		High density	
		p-value	R^2	p-value	R^2
MOE-d	Adhesive	0.5741	18.2	0.5380	3.1
	CNF	**0.0124**		0.4219	
MOR-d	Adhesive	0.8155	13.2	0.1011	9.4
	CNF	**0.0328**		0.4471	
Thickness Swelling	Adhesive	**0.0001**	75.6	**0.0001**	75.8
	CNF	0.0634		0.0611	
Water absorption	Adhesive	**0.0001**	44.1	**0.0001**	47.8
	CNF	0.1564		0.0637	
MOE-w	Adhesive	**0.0001**	50.8	**0.0001**	50.7
	CNF	0.2153		0.2062	
MOR-w	Adhesive	**0.0001**	39.9	**0.0001**	38.2
	CNF	0.4531		0.5708	
Internal bonding	Adhesive	**0.0001**	56.7	**0.0030**	27.9
	CNF	**0.0003**		0.1233	

Sample size 36 for each property

Low target density	High target density

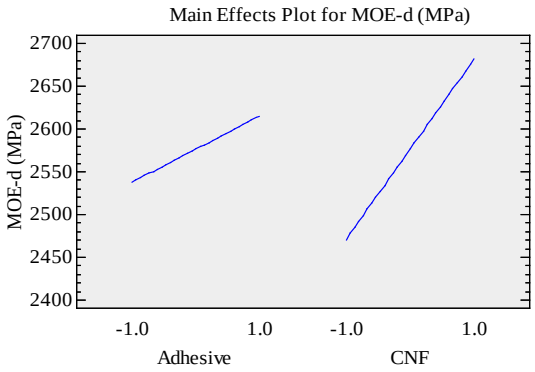

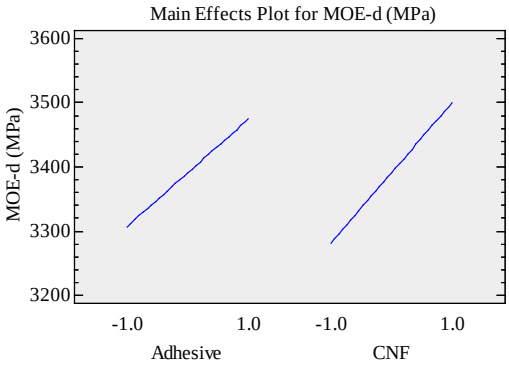

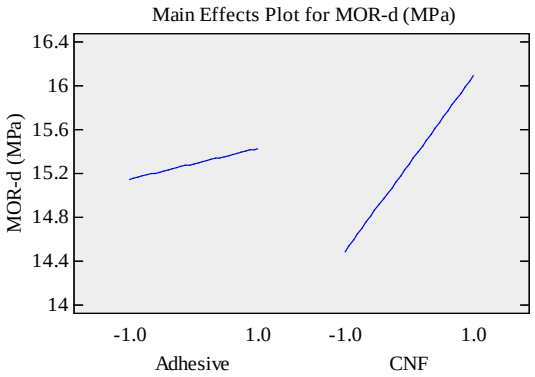

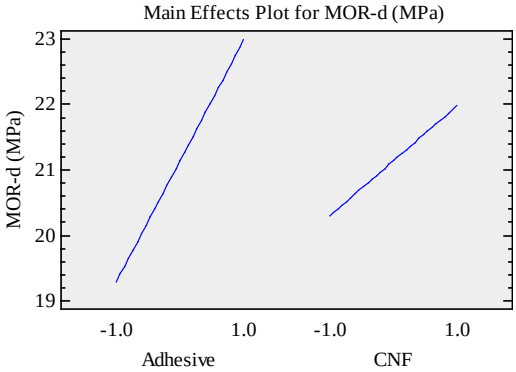

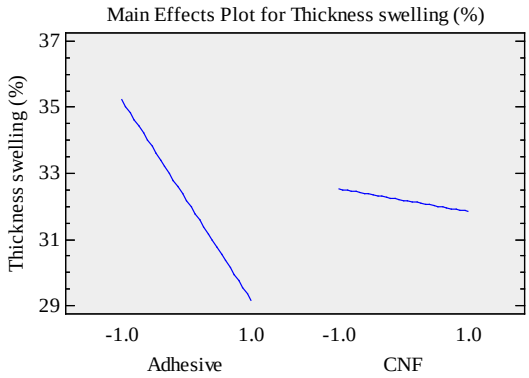

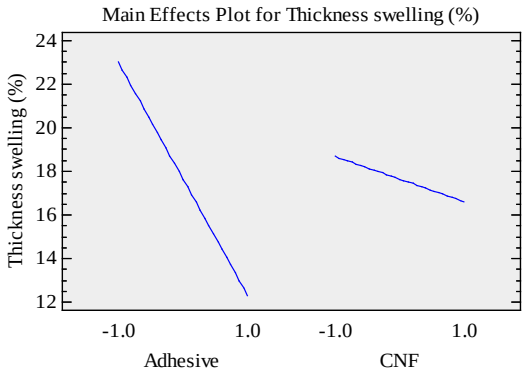

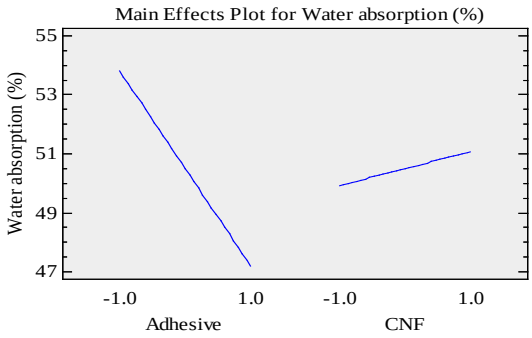

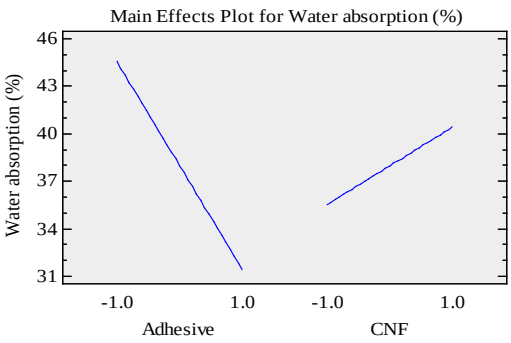

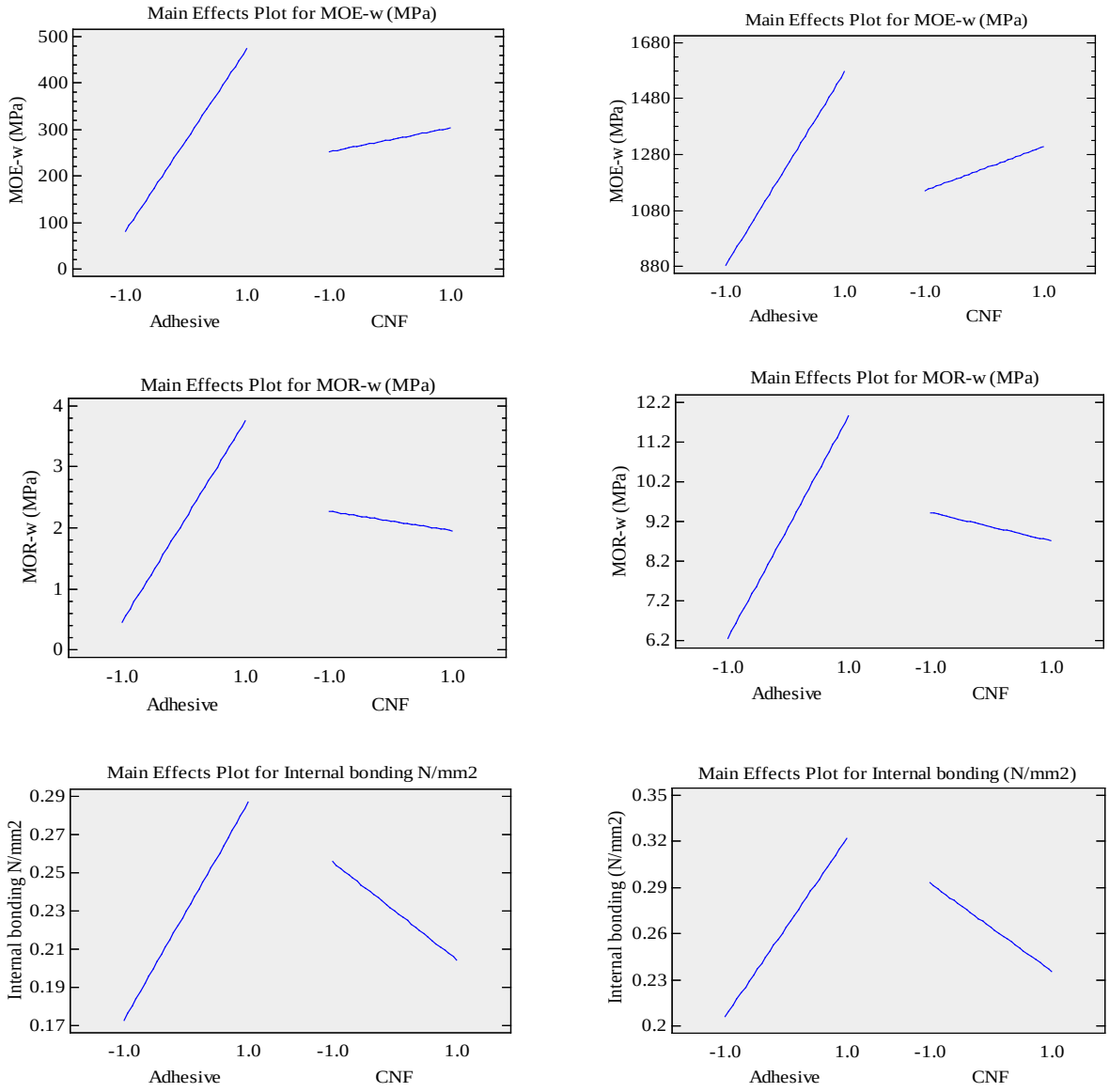

Figure 3.4. Comparison of the effect of adhesive and CNF in MOE-d, MOR-d, thickness swelling, water absorption, MOE-w, MOR-w, and internal bonding at low and high target density

3.3.2.2 Multiple linear regression including local density variation

Figure 3.5 displays the density of samples. As we can see, for the experimental design at target density 0.51 g/cm^3 and 0.60 g/cm^3, it was not possible to get this value for each sample. Therefore, a multiple linear regression in which apart of adhesive and CNF it was included the local density as an independent factor.

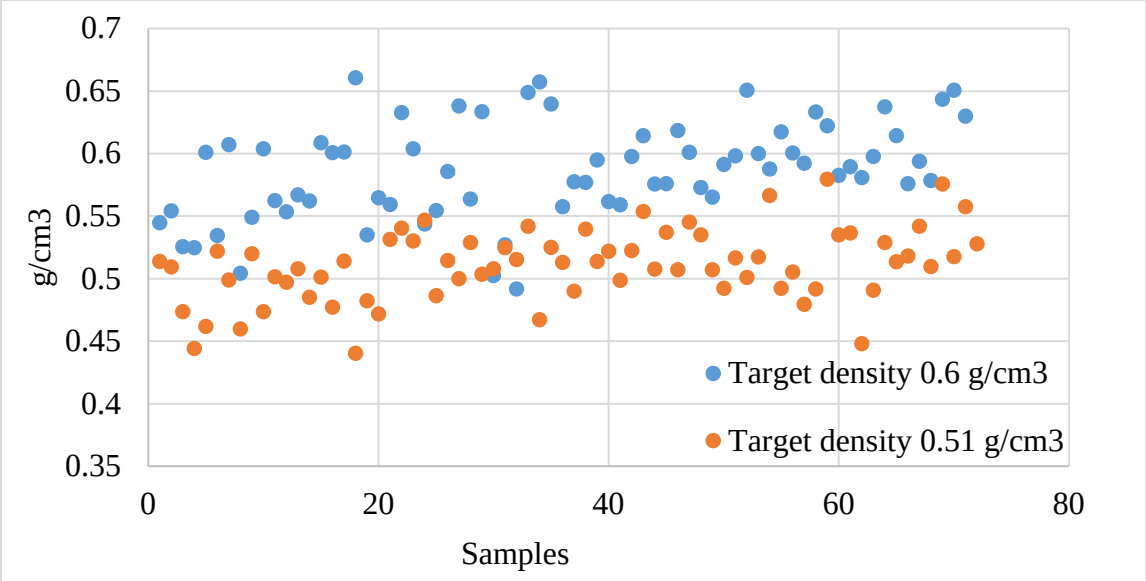

Figure 3.5 Range of density for low and high target density

Table 3.6 summaries the p-values of the adhesive, CNF and local density for MOE-d, MOR-d, MOE-w MOR-w, thickness swelling, water absorption, and internal bonding properties for the multiple linear regression at low and high target density. As it was found in the analysis without considering the local density, the adhesive had a significant effect on thickness swelling, water absorption, MOE-w MOR-w, and internal bonding at low and high target density. In all these properties, the more adhesive, the better the properties were.

The CNF had a significant effect on MOE-d and internal bonding at low target density, while at high target density the CNF had a significant effect on water absorption, and internal bonding. The positive effect of CNF in the MOE-d and the negative effect of CNF was already discussed in section 3.3.2.1. The negative effect of CNF in the water absorption properties could be due to free channel generated during the spring back caused by water and CO_2 at high temperatures.

The overall conclusion with and without including the local density as a factor was the same, but when the local density was included as a factor, the effect of CNF became to be relevant in the internal bonding and water absorption at high density.

Table 3.6. P-values for adhesive, CNF and local density factors at low and high target density from the multiple linear regression

Property	Independent variable	Low target density			High target density		
		p-value	R^2	Sample size	p-value	R^2	Sample size
MOE-d	Adhesive	0.5725	25.3	34	0.6590	43.0	35
	CNF	**0.0429**			0.5022		
	Local density	0.1035			**0.0002**		
MOR-d	Adhesive	0.1868	29.2	34	0.3439	43.9	35
	CNF	0.1428			0.6438		
	Local density	**0.0153**			**0.0004**		
Thickness Swelling	Adhesive	**0.0001**	72.4	33	**0.0001**	77.1	36
	CNF	0.1483			0.0506		
	Local density	0.4890			0.5402		
Water absorption	Adhesive	**0.0004**	41.0	33	**0.0001**	50.1	36
	CNF	0.1725			**0.0353**		
	Local density	0.9769			0.3025		
MOE-w	Adhesive	**0.0001**	45.1	33	**0.0001**	51.8	36
	CNF	0.3684			0.2631		
	Local density	0.8490			0.9809		
MOR-w	Adhesive	**0.0008**	34.1	33	**0.0001**	39.1	36
	CNF	0.5884			0.6841		
	Local density	0.7952			0.8255		
Internal bonding	Adhesive	**0.0153**	14.1	85	**0.0020**	20.1	69
	CNF	**0.0115**			**0.0150**		

3.3.3. Conclusion

The increment of adhesive had a significant effect on thickness swelling, water absorption, MOE-w MOR-w, and internal bonding at low and high-density panels. In all these properties, the more adhesive, the better the properties were. For MOE-d and MOR-d, at low and

high density the adhesive did not have a statistically significant effect at the 95.0 % confidence level.

The use of CNF showed a positive effect on MOE-d and MOR-d at low target density. For most of the properties, the partial replacement of pMDI by CNF did not have a statistically significant effect at the 95.0 % confidence level. Since partial replacement of pMDI by CNF did not have a statistically significant for most of the properties meaning that properties were not reduced, CNF could be an alternative to partial replace pMDI. However, CNF had a negative effect on internal bonding at the low and high-density panel. Therefore, more researches are necessary to overcome the issue of internal bonding reduction. It is believed that extra water added to the panel by the CNF substitution and CO_2 from the reaction between isocyanate group and water causes high internal pressure within the composite during the pressing step. The internal pressure could cause the spring back effect when the pressure from the press is removed and that could be the reason in the internal bonding reduction. To overcome the hypothesis that extra water reduces internal bonding, it was proposed for future work dewater the composite prior to pressing or to deliver the CNF with less water.

This conclusion was valid for laboratory board, therefore, the value of steam pressure, initial mat moisture content and pressing time optimized in the laboratory, should be reviewed when transferring the same system to industry.

References

ASTM. (2012). D1037 Standard Test Methods for Evaluating Properties of Wood-Base Fiber and Particle Panel Materials. American Society for Testing and Materials, West Conshohocken, PA.

Auad, L., Contos,V., Nutt, S., Aranguren, M. and Marcovich, N. (2008). Characterization of Nanocellulose- Reinforced Shape Memory Polyurethanes. Polymer International 57:651–59.

Heimbacha, F. Jaegerb, K., Sporenbergb, W. (1996). Fate and Biological Effects of Polymeric MDI. Ecotoxicology and Environmental Safety 33 (2):143–53.

Frihart, C. (2005). Wood adhesion and adhesives. Rowell RM, editor. Handbook of wood chemistry and wood composites. Florida: CRC Press. 215–78.

Hammett, A. and Youngs, R. (2002). Innovative Forest Products and Processes: Meeting Growing Demand. Journal of Forestry. 100 (4):6–11.

Imam, S., Gordon, S., Mao, L. and Chen, L. (2001). Environmentally Friendly Wood Adhesive from a Renewable Plant Polymer: Characteristics and Optimization. Polymer Degradation and Stability. 73:529–33.

Kamke. F., and Lee, J. (2007). Adhesive Penetration in Wood: A Review. Wood and Fiber Science. 39 (2):205–20.

Klemm, D., Kramer, F., Moritz, S., Lindström, T., Ankerfors, M., Gray D., and Dorris, A. (2011). Reviews Nanocelluloses: A New Family of Nature-Based. Angewandte Chemie - International Edition. 50:5438–66.

Kúdela, J., Rousek, R., Rademacher, P., Rešetka, M., and Dejmal, A. (2018). Influence

of pressing parameters on dimensional stability and density of compressed beech wood. Wood and Wood Products 76:1241–1252

Leventis, N., Sotiriou-leventis, C., Chandrasekaran, N., Mulik, S., Larimore, Z., Lu, H., Churu, G., Mang, J. (2010). Multifunctional Polyurea Aerogels from Isocyanates and Water. A Structure - Property Case Study. Chemistry of Materials 22:6692–6710.

Mäkinen, H., Saranpää, P. and Linder, S. (2002). Wood-Density Variation of Norway Spruce in Relation to Nutrient Optimization and Fibre Dimensions. Canadian Journal of Forest Research. 32:185–94.

Manwiller, G. (1972). Tracheid Dimensions in Rootwood of Southern Pine. Wood Scientist, USDA Forest Service.

Mi-Jung, C. and Byung-Dae, P. (2011). Tensile and Thermal Properties of Nanocellulose Reinforced Poly Vinyl Alcohol. Industrial and Engineering Chemistry 17(1):36–40.

Niyogi, D., Kumar, R., and Gandhi, K. (1999). Water Blown Free Rise Polyurethane Foams. 39(1):199–209.

Nugroho, N., Ando, N. (2000) Development of structural composite products made from bamboo I: fundamental properties of bamboo zephyr board. J Wood Science 46:68–74

Pizzi, A. (1994). Advanced wood adhesives technology. CRC Press.

Xiaobin, L., Hongbin, C., and Yi, Z. (2007). Structures and Physical Properties of Rigid Polyurethane Foams with Water as the Sole Blowing Agent. Science in China Series B: Chemestry 49(4):363–70.

Zimmermann, T., Bordeanu, N. and Strub, E. (2010). Properties of Nanofibrillated Cellulose from Different Raw Materials and Its Reinforcement Potential. Carbohydrate Polymers 79(4):1086–1093.